# Survival in a sea of gradients:
# Bacterial and archaeal foraging in a heterogeneous ocean

Estelle E. Clerc[1], Jean-Baptiste Raina[2], François J. Peaudecerf[1], Justin R. Seymour[2], Roman Stocker[1]*

[1] Institute of Environmental Engineering, Department of Civil, Environmental and Geomatic Engineering, ETH Zurich, Switzerland

[2] Climate Change Cluster, University of Technology Sydney, Sydney, Australia

*Corresponding author: romanstocker@ethz.ch

Table of contents

# 1. Introduction

The marine environment is one of the largest reservoirs of bacteria and archaea on Earth, with each liter of seawater containing approximately 1 billion cells. Latest estimates suggest that a total of $10^{29}$ bacteria and archaea populates the world's ocean (Kallmeyer et al., 2012), accounting for ~70% of the total marine biomass (Bar-On et al., 2018). This abundance encompasses a wide phylogenetic diversity and a broad range of trophic strategies (Lauro et al., 2009). At one end of the trophic spectrum, oligotrophs are adapted to environments with low levels of nutrients and these microorganisms are characterized by slow growth, low metabolic rates, small cell sizes, streamlined genomes, and a lack of motility (Overmann and Lepleux, 2016). Some, such as *Pelagibacter ubique*, numerically dominate open ocean communities (Giovannoni, 2017) and need only few specific nutrients to grow (Carini et al., 2013; Tripp et al., 2008). In the nutrient-poor waters they inhabit, oligotrophs rely on molecular diffusion, which brings enough nutrients to their contact to sustain growth (Zehr et al., 2017). At the other end of the trophic spectrum, copiotrophs thrive in nutrient-rich environments. They grow rapidly, have high metabolic rates, large cell sizes, possess larger genome sizes, and are often motile. In addition, they are well equipped to sense, integrate and respond to extracellular stimuli (Lauro et al., 2009), allowing them to find and exploit nutrient patches and hotspots. Although copiotrophs represent a small percentage of the free-living microorganisms in the open ocean, they account for most of the organisms on sinking particles (Lambert et al., 2019). While oligotrophy and copiotrophy are often represented as a dichotomy, there is in fact a continuum of trophic strategies between these extremes (Lauro et al., 2009), which enables a wide diversity of microorganisms to exploit hotspots of nutrients in the ocean.

The environment experienced by individual microbial cells in the water column is surprisingly heterogeneous, punctuated by chemical patches and pulses, as well as sinking and suspended organic particles (Azam, 1998; Stocker, 2012). This microscale heterogeneity influences the behavior, physiology, and trophic interactions of microorganisms and ultimately impacts their contribution to biogeochemical cycles (Azam and Long, 2001; Smriga et al., 2016; Stocker et al., 2008). Yet, recognition of this heterogeneity and its importance is only recent. As a result, the ecology of marine bacterial and archaeal communities has only rarely been studied at scales that reflect the microscale environments experienced by these organisms. Indeed, microbial processes within the pelagic ocean are traditionally investigated over large spatial and temporal scales, under the assumption that planktonic organisms and solutes are homogeneously mixed by turbulence. Consequently, patterns in microbial abundance, activity and diversity have most commonly been examined in the context of mesoscale oceanographic features (e.g., currents, eddies, gyres) or large-scale gradients (e.g., temperature, salinity) using bulk sampling

techniques such as Niskin bottles that collect liters of seawater. However, multi-liter seawater samples exceed the scales of important microscale features and microbial interactions by over 1 million-fold in volume. To draw a parallel, this would be equivalent to studying the foraging behavior of coral reef fishes by sampling them with a device 100 times larger than an oil supertanker.

Evidence has confirmed that many marine bacteria and archaea are well equipped to navigate and exploit the heterogeneous seascape they inhabit (Blackburn et al., 1998; Brumley et al., 2019; Son et al., 2016; Stocker et al., 2008), emphasizing the importance of studying these organisms at the appropriate scale and the need to integrate the effects of microscale gradients into studies of marine microbial ecology. The few studies that have examined the distribution and diversity of marine microbes at sub-centimeter scales have revealed that bacterial abundances in localized hotspots can be an order of magnitude higher than background (Seymour et al., 2000), that microscale patchiness exists in species richness (Long and Azam, 2001), and that marine bacteria and archaea can use motility and chemotaxis to aggregate in microscale nutrient hotspots (Fenchel, 2001; Lambert et al., 2017; Mitchell et al., 1996). Although these fine-scale field results are consistent with theoretical predictions (Azam, 1998; Kiørboe and Jackson, 2001) and laboratory studies (Blackburn et al., 1998; Smriga et al., 2016; Stocker et al., 2008), they are rare, and our perception of the life of a microbe in the ocean is only beginning to emerge. In this chapter, we consider the pelagic ocean from the perspective of a planktonic microorganism, by describing the microscale physics of seawater, the chemical and biological phenomena that define microscale seascapes, and the behavioral and physiological adaptations that permit marine microbes to succeed in this patchy and dynamic world.

## 2. The physics of marine microenvironments

While the ocean represents an incredibly complex environment at the microscopic scale, rich with a multitude of nutrient sources and microbial species, our understanding of the physics at play enables us to establish some general principles. In this section, we outline how two key physical drivers, namely molecular diffusion and fluid flow, define marine microenvironments in terms of nutrient concentration dynamics. We then present some general considerations of the challenges and opportunities for bacteria in the resulting resource seascape, with the overall goal of providing an intuition about microbial processes at the microscale.

### 2.1 Diffusion and flow shape microscale nutrient seascapes

Molecular diffusion is the key physical phenomenon that shapes the chemical seascape at the microscale. In the absence of flow, even an initially localized release of nutrients, for example from a lysing cell, will result in a slowly extending patch, as thermal agitation at the molecular scale disperses the resource. This patch of nutrient will thus be smoothed out progressively over time until it reaches the level of background concentration, at which point it becomes difficult for copiotrophic bacteria to exploit. Typically, for a molecule with diffusivity $D$, a point source spreads to a distance $L = (6Dt)^{1/2}$ after a time $t$. As this scaling law shows, the rate of expansion ($dL/dt = (3D/2t)^{1/2}$ will decrease with time, and is set by the compound's diffusivity $D$. Considering a typical diffusivity of $D = 0.5 \times 10^{-9}$ m$^2$/s for small molecules, a point source will become a patch of 250 μm diameter in 20 s and of 2 mm diameter in 20 min. As the patch expands with time, the gradients of concentration at its edges become smaller, as do the peak and mean concentrations of the patch which scale as $t^{-3/2}$ (Fig. 1a,b) (Berg, 1993; Blackburn et al., 1997; Jackson, 2012). For example, the concentration of a compound originating from a lysing event from a cell of radius $R$ will be diluted 1000-fold relative to the intracellular concentration when the pulse has expanded to a distance $L = 10R$, which occurs over a typical time $t = (10R)^2/6D$, or ~20 s for $R = 25$ μm and $D = 0.5 \times 10^{-9}$ m$^2$/s. The time to dilution will thus vary strongly between lysing cells of different sizes (Fig. 1c).

The dependence of the timescale for diffusive spreading on the diffusivity of the solute means that different compounds will not diffuse at the same rate: high-molecular-weight compounds diffuse more slowly than their smaller dissolved counterparts, and will generate more persistent gradients (Stocker and Seymour, 2012). For instance, the diffusivity of the small dissolved monomer glucose is $D = 0.5 \times 10^{-9}$ m$^2$/s (Ziegler et al., 1987), whereas the large polysaccharide laminarin is $D = 1.5 \times 10^{-10}$ m$^2$/s (Elyakova et al., 1994), demonstrating the variability of molecular diffusivities found in organic compounds. As the content of a cell is a rich cocktail of many substances (Hellebust, 1965) that diffuse at different rates, the lifetime and dynamics of a nutrient pulse from a cell lysing event depends on the molecular composition of the cell's cytoplasm. Overall, diffusion will smooth out any localized and transient source of nutrient into the background concentration. As we discuss below, active foraging of copiotrophic bacteria can, among other benefits, provide a way to cope with this need for timely exploitation of resources before they disappear.

Diffusion also governs the nutrient profiles around sources of nutrients with a steady release, such as live phytoplankton cells with a constant leakage of photosynthates (Fig. 1d; Bell and Mitchell, 1972; Blackburn et al., 1998; Cirri and Pohnert, 2019; Seymour et al., 2017; Smriga et al., 2016). In this case, in the absence of flow and without strong uptake by other cells, a steady decreasing nutrient profile is

established by diffusion around the algal cell (Fig. 1e), with concentration inversely proportional to the distance from the center of the cell (Kiørboe et al., 2002). The microenvironment immediately surrounding phytoplankton cells is known as the phycosphere, it is characterized by a concentration of nutrients higher than the bulk seawater but also by its bacterial accumulation potential (Bell and Mitchell, 1972; Cole, 1982; Seymour et al., 2017; Stocker, 2012) and represents one of the most well-studied nutrient hotspots in the ocean (Azam and Malfatti, 2007; Mühlenbruch et al., 2018; Thornton, 2014). The extent of the phycosphere increases with the size of the phytoplankton cell and typically extends over a few cell radii. For example, for a phytoplankton of radius 10 µm, the above-background nutrient concentration will typically establish over 20 to 50 µm (Fig. 1f).

Steady diffusive profiles can also be found emanating from the surface of large organisms leaking nutrients, such as corals or sponges, and from the sediment–water interface. At these interfaces, the nutrient concentration decays with distance from the surface. Specifically, assuming a constant and uniform release rate (for example, of hydrogen sulfide from the sediment surface), molecular diffusion will spread the nutrient away from the surface according to a linear concentration gradient extending a fraction of a millimeter (0.1 to 1 mm) into the water (Schulz and Jørgensen, 2001).

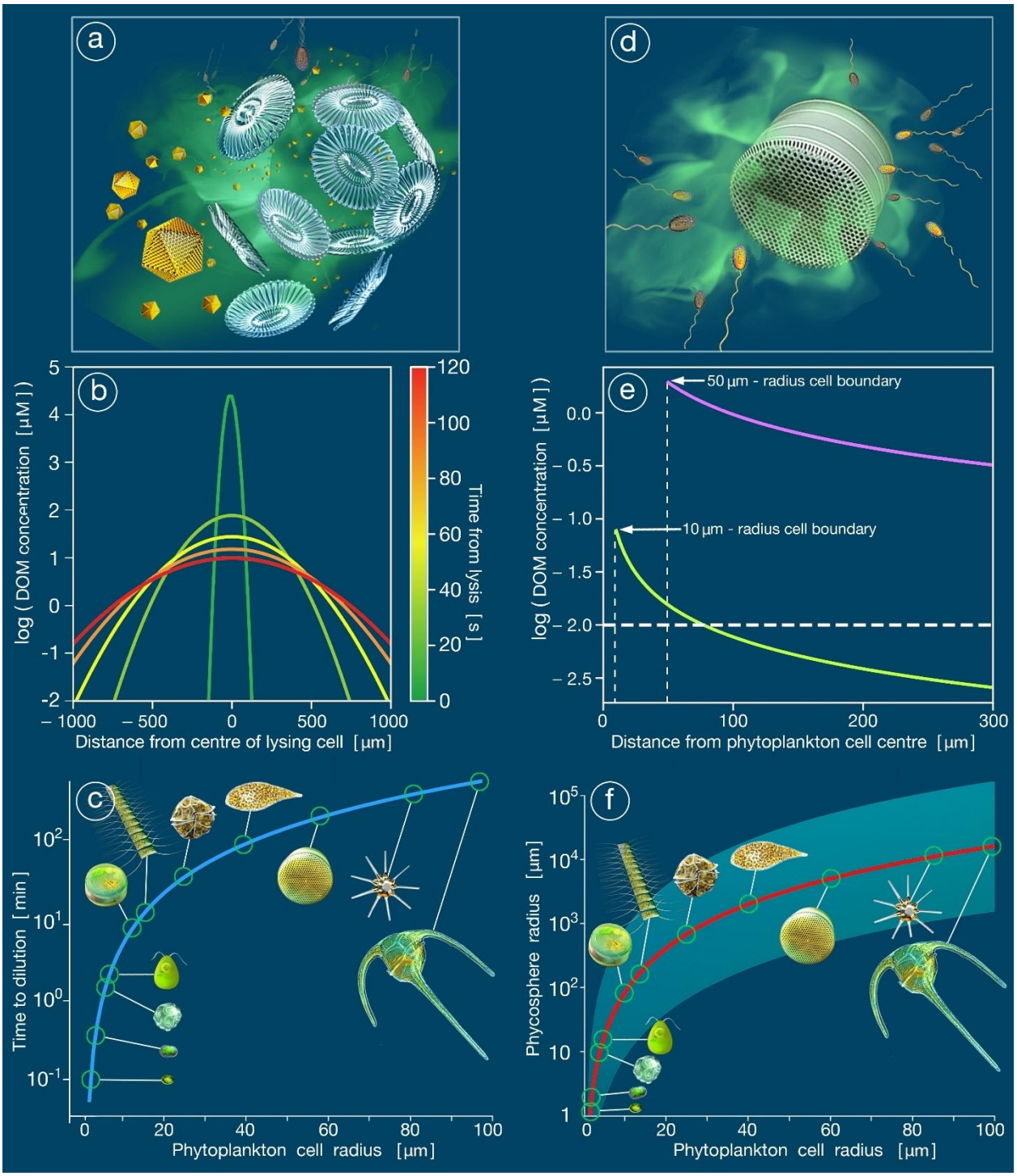


**Figure 1**. Ephemeral (lysing events) and permanent (phycosphere) nutrient patches from algal cells. (**a**) An artist's impression of the lysis of a phytoplankton cell, resulting in a strong yet ephemeral pulse of dissolved organic matter (DOM). (**b**) The DOM concentration field as it evolves over time after a lysis event. Concentration was computed using a mathematical model of diffusion from a pulse source, following Seymour et al. (2010a). The horizontal axis shows the distance from the center of a lysing cell

of radius 25 μm, which bursts open at time 0, releasing an intracellular concentration of 100 mM of a small-molecule compound (diffusivity $0.5 \times 10^{-9}$ $m^2/s$). (**c**) Scaling of the time to dilution of a lysis patch for different phytoplankton sizes. The intracellular concentration was set to 100 mM with diffusivity $D = 0.5 \times 10^{-9}$ $m^2/s$. For each cell size, the size of the patch grows as $L = (6Dt)^{1/2}$ and is considered diluted when its average concentration has reduced to 10 times the background concentration of 10 nM. (**d**) An artist's impression of the diffusion boundary layer around an individual phytoplankton cell, which incorporates the phycosphere where concentrations of DOM are enhanced over background level. (**e**) The decay of DOM concentration with distance from the center of a DOM-exuding phytoplankton. Concentrations are shown for phytoplankton of two different radii: 10 μm (bottom light green curve) and 50 μm (top magenta curve). The black dashed line shows a bulk background concentration of 10 nM (typical of many organic solutes in the ocean). The DOM concentration fields were obtained by solving the steady diffusion equation for a constant source, following Seymour et al. (2010a). The phytoplankton cell was assumed to have an intracellular concentration of 100 mM, a 1-day typical doubling time, and to exude 100% of its daily production of the solute. This upper limit for the exudation rate is most applicable to stressed or senescent cells. The diffusivity for the solute was $D = 0.5 \times 10^{-9}$ $m^2/s$. (**f**) Phycosphere radius as a function of cell radius. The red line corresponds to the size of the region around a cell where the concentration of a specific compound is >50% above background, shown here for a compound with diffusivity of $D = 0.5 \times 10^{-9}$ $m^2/s$, a leakage fraction of 5%, a phytoplankton growth rate of one per day, and a background concentration of this compound of 10 nM. The light-blue shaded region shows the variation of the phycosphere size when exudation rate is 10 times lower to 10 times higher. The cells presented on panels (c) and (f) are, from smaller to larger, *Prochlorochoccus*, *Synechococcus*, *Emiliania*, *Chlamydomonas*, *Thalassiosira*, *Chaetoceros*, *Alexandrium*, *Chattonella*, *Coscinodiscus*, *Asterionellopsis*, *Ceratium*.

These characteristics of nutrient sources, both the transient hotspots linked to sudden release of nutrients and the more stable nutrient profiles around steady sources, were established considering only diffusive transport. The resulting size of these hotspots and gradients within them directly influence microbial foraging, for example by determining growth of microbes able to localize within phycospheres and the gradients that chemotactic microbes can exploit to seek phytoplankton cells. One would intuitively think that fluid flow and turbulence in the ocean significantly modify these nutrient profiles. It turns out that at the microscale, the mixing effect of turbulence remains subordinate to diffusion in governing the concentration of nutrients. If we consider an initial nutrient patch on the scale of millimeters to centimeters (Fig. 2), turbulence will stir, stretch, and fold the patch into thin sheets and filaments (Taylor and Stocker, 2012). As a consequence, turbulence initially enhances heterogeneity at the microscale.

These fine structures become progressively smaller, down to the Batchelor scale (Box 1), which typically ranges from 30 to 300 μm in the ocean (Guasto et al., 2012). As even very large sources of solute are ultimately stirred into Batchelor-scale filaments and sheets, the Batchelor scale provides a universal scaling for microbial oceanography (Stocker, 2015). For any patch smaller than this scale, turbulence will not fragment the profile formed by diffusion, but will simply stretch it. The importance of this deformation relative to pure diffusion is captured by the turbulent Péclet number (Box 2, (Guasto et al., 2012)).

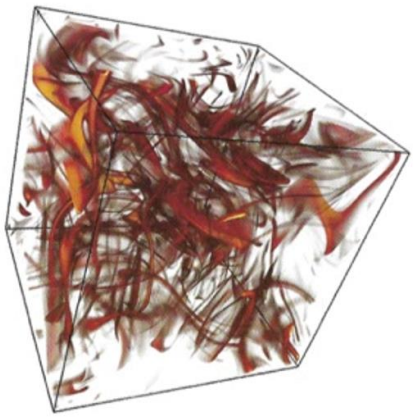

**Figure 2**. Turbulence can contribute to patchiness and heterogeneity. The cube represents a numerical simulation of the effect of turbulence on a patch of dissolved organic matter (DOM), with shading indicating the DOM concentration. Turbulence stretches, folds, and stirs the initial DOM patch to create a tangled web of sheets and filaments as small as the Batchelor scale (30 to 300 μm in the ocean). The characteristic timescale of this process, for a 2.5 mm patch in moderately strong turbulence (turbulent dissipation rate = $10^{-6}$ W/kg), is in the order of 1 min. The computational domain size is 5.65 cm (Taylor and Stocker, unpublished).

***Box 1**: The Batchelor scale*

The Batchelor scale, $L_B = (\nu D^2/\varepsilon)^{1/4}$, is the lowest scale at which turbulence can generate variance in the distribution of nutrients. Below this size, molecular diffusion dissipates gradients, thereby truly mixing solutes. Here, $\nu = 10^{-6}$ m$^2$/s is the kinematic viscosity of water, $D$ is the solute's diffusivity, and $\varepsilon$ is the turbulent dissipation rate, characterizing the intensity of turbulence. The Batchelor scale $L_B$ increases with diffusivity, and decreases with increasing dissipation rate. For typical marine

conditions, the turbulent dissipation rate ε varies between $10^{-6}$ and $10^{-10}$ W/kg, which for small molecules (D ~ $10^{-9}$ $m^2$/s) corresponds to $L_B$ = 30 μm to 300 μm (Guasto et al., 2012).

***Box 2**: The Péclet number*

The Péclet number Pe is a non-dimensional parameter estimating the ratio of the magnitude of transport by both flow and molecular diffusion, characterizing how important each mechanism is at moving nutrients around an object. If Pe < 1, diffusion is the dominant mechanism of transport and flow plays a lesser role in the formation of nutrient concentration profiles. Its general expression Pe = $UR/D$ depends on a typical speed $U$, a typical size $R$, and the diffusivity of the solutes $D$. For example, for a small patch of size $R$ in turbulence with dissipation rate ε, the typical speed will be $R(\varepsilon/\nu)^{1/2}$ and thus Pe = $R^2(\varepsilon/\nu)^{1/2}/D$ will quantify how much turbulence deforms this patch from its purely diffusive shape. Strong turbulence (ε = $10^{-6}$ W/kg) acting on a patch of small molecules (D ~ $10^{-9}$ $m^2$/s) of radius $R$ = 50 μm thus results in Pe = 2.5, characteristic of a strong deformation of the patch by the turbulent flows. Alternatively, a particle of size $R$ sinking at speed $U$ will have an associated Pe = $UR/D$ that will determine the shape of its plume (Fig. 3, (Guasto et al., 2012; Kiørboe and Jackson, 2001; Stocker et al., 2008)).

Turbulence also impacts the nutrient profiles resulting from solid surfaces. In this situation, turbulence does not mix freely, but is damped by the presence of the surface. The region close to the surface where turbulence is quenched and diffusion dominates transport is called the "diffusion boundary layer" (DBL, (Schulz and Jørgensen, 2001; Thar and Kühl, 2002)). DBLs can be found around all solid surfaces in the ocean, from corals to sediments, and they also surround marine snow particles and phytoplankton cells. The diffusive transport results in mostly steady gradients of solute, providing a robust clue of the location of the source to chemotactic microorganisms. The stronger the surrounding flow, the thinner the DBL, and hence the greater the solute transport to and from the surface (for example over corals in flow (Kühl et al., 1995)). For phytoplankton cells, the phycosphere as described above corresponds generally with the DBL (Seymour et al., 2017).

Finally, the shape of the nutrient seascape in the ocean is also strongly determined by the sinking motion of leaking objects, such as marine snow particles and fecal pellets (Kiørboe and Jackson, 2001). As they move through the water column while releasing solutes, marine snow particles and fecal pellets generate a quite different nutrient signature from the static diffusive sources described above, as what would be a spherical DBL is deformed into a comet-like plume. The concentration seascape they generate is strongly asymmetric with a thin layer of higher concentration characterized by strong gradients preceding these

particles and a long solute tail with concentration higher than background in their wake (Kiørboe and Jackson, 2001; Stocker et al., 2008). This asymmetry, and thus the slenderness of the plume, increases with increasing Péclet number, and thus for example with increasing sinking speed (Box 2 and Fig. 3). This plume is itself subject to diffusion and turbulence and ultimately becomes diluted in the background (Kiørboe and Jackson, 2001; Visser and Jackson, 2004).

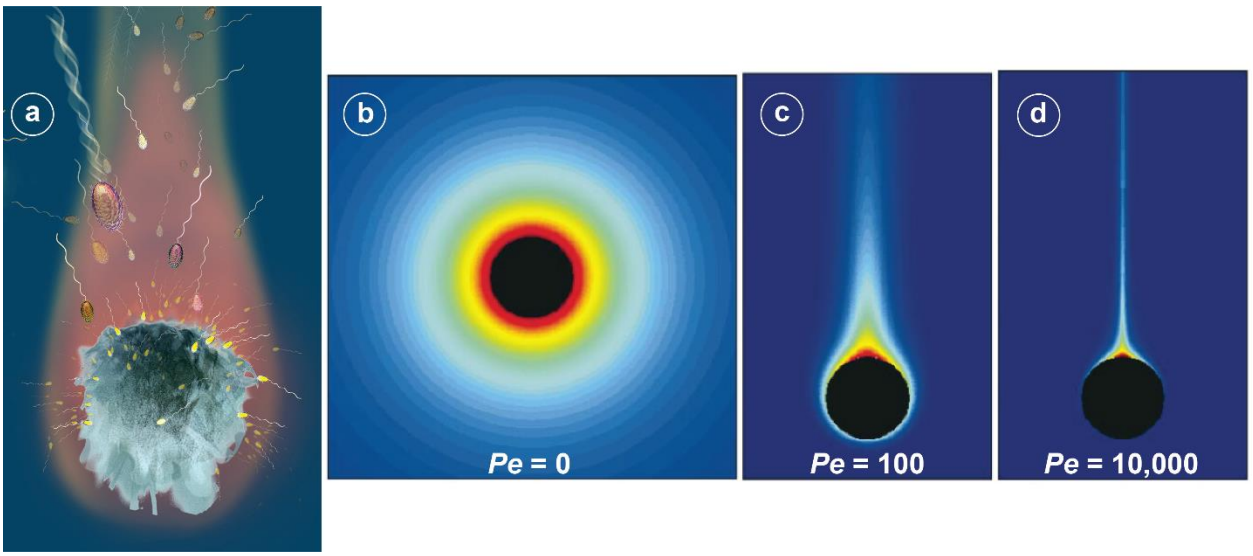


**Figure 3**. Marine particles. (**a**) An artist's impression of the plume of dissolved organic matter emanating from a sinking marine snow particle. (**b-d**) The shape of the plume for sinking particles of different Péclet number. The Péclet number Pe = *UR*/*D* for a particle of size *R* releasing a solute of diffusivity *D* and sinking at speed *U* characterizes the importance of flow in shaping the plume with respect to pure diffusion (Pe = 0). Shown are plumes for Péclet numbers of (**b**) Pe = 0, (**c**) Pe = 100 and (**d**) Pe = 10,000, corresponding to a static particle, a slow sinking particle, and a fast-sinking particle, respectively. Reproduced from Kiørboe et al. (2001), with permission.

## 2.2 A bacterial view of the microscale ocean

Physical phenomena define the chemical seascape at the microscale, resulting in a heterogeneous mosaic of transient hotspots amidst otherwise nutrient-poor waters. To understand the value of microbial behaviors, such as motility and chemotaxis, to navigate this seascape of resources, it is useful to picture the typical distances between cells in the ocean, as these distances have direct implications for the rates at which bacteria might expect to encounter, for example, a phytoplankton cell. If we take a typical concentration of bacteria of $10^6$ cells/mL — a relatively conserved value across the world's ocean — and distribute these cells uniformly in space, then the distance between a bacterium and its nearest neighbor

would be 100 μm, i.e. ~100 body lengths. This separation does not change much with small changes in cell concentration, as it varies with the cubic root of the cell density (for example, $10^5$ cells/mL corresponds to a nearest neighbor distance of roughly 200 μm). Regarding the typical distance of these bacteria from potential sources of nutrients at the microscale, consider again a bacteria concentration of $10^6$ cells/mL together with a phytoplankton population at a typical cell density of $10^3$ cells/mL, both uniformly distributed. Then, for each individual bacterium, the nearest phytoplankton cell is at a distance of the order of 1 mm. Once again, this distance hardly varies with small variations in cell density. Overall, these considerations paint a picture of the ocean as a dilute suspension of microorganisms, with bacteria separated by many cell diameters from other bacteria and potential nutrient sources such as phytoplankton cells.

How can bacteria then find their way to nutrient hotspots? In the absence of motility, bacterial cells are subjected to Brownian motion, the small fluctuations in position driven by random collisions with water molecules. Brownian motion of a bacterium can be quantified by the diffusivity $D_B = kT/(6\pi\mu R)$ which is inversely proportional to bacterial radius $R$ and proportional to temperature $T$, with other parameters $k$ Boltzmann's constant and μ the dynamic viscosity of seawater. For typical seawater conditions at 10°C, $D_B$ is of the order of $3.5 \times 10^{-13}$ m$^2$/s for a bacterium of radius 0.4 μm. As a result of the random path they follow by Brownian motion, non-motile bacteria will cover a typical distance $L = (6D_Bt)^{1/2}$ in a time $t$. These distances are small: for example, $L \sim 35$ μm in 10 minutes and $L \sim 450$ μm in one day. These values suggest that over the timescale of a day, a bacterium might encounter another bacterium. However, if we ask how long it would take to cover the typical separation with a phytoplankton cell $L \sim 1$ mm, the estimated time rises to $t \sim 6$ days (Smriga et al., 2016). This timescale is not only large compared to the doubling time of the bacterium, which could thus begin to starve during its random search, but it is also large compared to the lifetime of a transient hotspot of nutrients. For example, the mean concentration of an algal lysis patch with initial size $R = 25$ μm for a small nutrient with $D = 0.5 \times 10^{-9}$ m$^2$/s decreases from an intracellular concentration of 100 mM (10 million times the background concentration of 10 nM) to 100 nM (just 10 times the background concentration) after around 30 min. Therefore, in most cases, random motion by Brownian diffusion will not increase the chances of non-motile bacteria encountering transient nutrient sources beyond the rare case of a hotspot arising near them by chance (Fig. 4a) (Smriga et al., 2016).

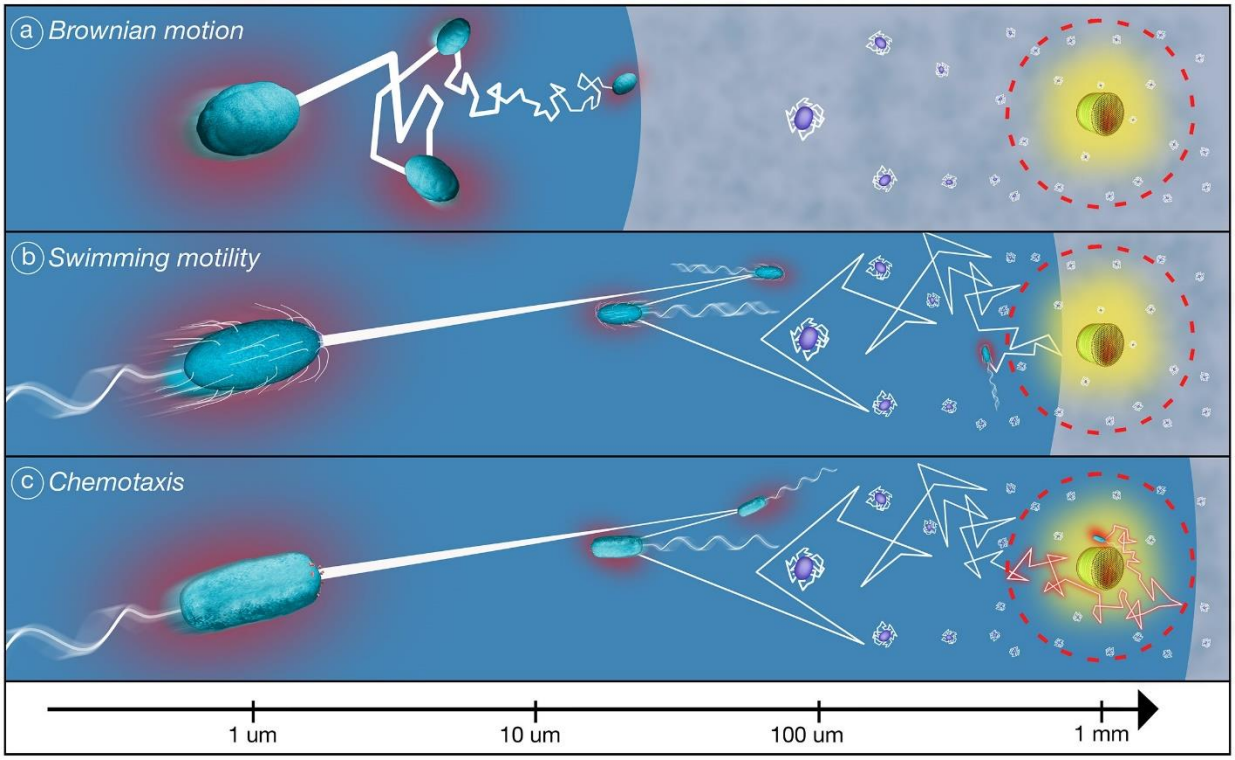


**Figure 4.** Different motility strategies result in different probabilities of encounter with other cells and nutrient hotspots. (**a**) Non-motile bacteria diffuse randomly driven by Brownian motion, with small domains explored in an example timescale of 10 min, giving a low probability of encountering other bacterial cells, and an even lower probability of entering a phycosphere (dashed line around phytoplankton cell). (**b**) Motile bacteria swim with a random pattern alternating straight runs and random reorientation. This more rapid random walk allows them to explore much larger domains, with the potential for many encounters with other bacteria and the potential "lucky" encounter with a phycosphere. (**c**) Chemotactic bacteria swim with the same random motion in the absence of a nutrient gradient. However, as soon as they detect a patch of higher nutrient concentration (e.g., entering the phycosphere marked by a dashed line), their random walk becomes biased toward the source, thus enabling them to rapidly navigate to the center of a nutrient patch and retain position there (red path).

We can actually estimate the encounter rate between microbes more precisely, based on their respective sizes and diffusivities. If we consider one bacterial cell (having radius $r$ and Brownian diffusivity $D_B$) and ask how often it is expected to encounter an algal cell (of radius $R$, Brownian diffusivity $D_{B,a}$, and cell concentration $C_2$), the average encounter rate will be given by $4\pi(D_B + D_{B,a})(r + R)C_2$, in cells encountered per day. If we consider non-motile bacteria of radius $r$ = 0.4 μm, and algal cells of radius $R$ =

25 μm and cell concentration $C_2 = 10^3$ cells/mL, on average one bacterium will encounter 0.01 algal cells over the course of a day, making the probability of arriving at the time of a lysis event very small.

Given the typical length scales and timescales that characterize the heterogeneous seascape of nutrients at the microscale, random Brownian motion is thus not an effective strategy to exploit transient nutrient hotspots. In contrast, bacterial motility, a feature of most copiotrophic bacteria, represents a game changer. Swimming bacteria possess one or several corkscrew-shaped flagella that they rotate to move through fluids (the characteristics and distribution of motility in marine bacteria are described in section 4). The resulting motion achieves typical speeds of 50 μm/s, with some species measured at speeds as fast as several hundred micrometers per second (e.g. large sulfur bacteria living above sediment such as *Thiovolum majus* (Fenchel, 1994)) which represents several hundredths of body lengths per second. This fast-swimming motion does not follow a straight line: similarly to the run-and-tumble motion of the enteric bacterium *Escherichia coli*, marine bacteria often alternate straight "runs" with random reorientations (described in section 4). This motility pattern, like Brownian motion, results in a random walk in space, but the greater magnitude of displacements greatly increases the volume explored by bacterial cells and thus their chances of encountering resources.

Indeed, a bacterial diffusivity $D_b$ (not to be confused with Brownian diffusivity) can be computed from the pattern of bacterial motion. When tracking in three dimensions the displacement $r(t)$ of a bacterium with time (i.e. the distance covered from its original position), the mean square displacement $\langle r(t)^2 \rangle$ (where angular brackets denote a mean over several choices of time origin) for a randomly swimming cell will evolve linearly with time after a timescale $t$ of a few seconds, the slope being equal to $6D_b$, with $D_b$ the bacterial diffusivity linked to random motility. This diffusivity is ranging typically from $5 \times 10^{-10}$ m$^2$/s to $8 \times 10^{-9}$ m$^2$/s (Kiørboe, 2008), so varying at most by one order of magnitude between bacterial species. From this bacterial diffusivity, one can determine the typical lengths explored by a swimming bacterium. During a time $t$, the size of the domain explored by a randomly swimming bacterium is once again given by the scaling $L = (6D_b t)^{1/2}$ (similar scaling as for Brownian motion but now with bacterial diffusivity in the place of Brownian diffusivity). Using a bacterial diffusivity $D_b = 10^{-9}$ m$^2$/s, we thus deduce that a motile bacterium explores a domain of typical size $L \sim 2$ mm in 10 min and size $L \sim 2$ cm in a day! This is almost 50 times larger than the distance that could be reached by purely passive Brownian diffusion, and the volume explored is correspondingly greater by a factor of $50^3$. Moreover, using the diffusive encounter rate formula above replacing Brownian diffusivity $D_B$ by swimming diffusivity $D_b = 10^{-9}$ m$^2$/s reveals that these motile bacteria would now on average encounter around 25 algal cells (of radius $R = 25$ μm and at a cell concentration of $10^3$ cells/mL) over the course of one day (note that more precise

estimates would require a fuller model of encounter than the simplified diffusive process used here as a first approximation). Motility thus greatly increases the chances of bacteria encountering other cells or nutrient hotspots (Fig. 4b) (Lambert et al., 2019). The possibility to reach a transient resource such as a lysing algal cell, or a sinking particle, is significantly enhanced by motility, and the rewards associated with these rich nutrient sources could explain the preservation of this behavior in the oceans, where the background concentration of nutrient can be very low (as described below).

It should be noted that this description of random encounters, while providing an idea of the time and length scales at play, represents a simplification with regards to natural systems, in which other parameters such as cell shape and flow could also influence successful encounters. For example, it has been shown that elongated motile bacterial cells can be reoriented by the flow around a sinking particle. This interaction with flow can reorient cells so that their initially random swimming direction ends up facing the particle, favoring their arrival onto the particle and thus increasing the number of successful encounters (Slomka et al., 2020). The characterization of bacterial encounters in the ocean in general has many facets that await study, and we foresee many potential developments in this area.

We have up to here considered only random encounters, based on either Brownian motion or random bacterial motility. However, a large number of motile bacteria are also chemotactic, which means that they can sense gradients of certain nutrients and move in the direction of higher concentrations (behavior described in detail in section 4). This chemotactic behavior is achieved by incorporating a bias into the random swimming pattern described above. Bacterial cell bodies are generally too small to be able to sense a gradient of nutrients over their cell length, with only few known exceptions for larger bacteria (Thar and Kühl, 2003). Therefore, chemotaxis occurs by sensing how the local concentration varies during a straight run. If the bacterium senses an increasing concentration, the run lasts longer; in contrast, if it senses a decreasing concentration, it tends to "tumble" and change direction earlier. The net result of these longer runs toward higher concentration is a general drift of the bacterium toward higher concentrations, such as the center of a nutrient patch or a phycosphere (Fig. 4c). Therefore, a chemotactic bacterium does not rely upon randomly moving to the center of a nutrient patch, as above for the random motility case. As bacteria can sense small concentration differences, a bacterium simply needs to randomly encounter the gradients of concentrations at the edge of a nutrient patch and then chemotaxis allows it to quickly swim toward the center of the patch to reach the highest nutrient concentrations. As diffusion disperses nutrients over large distances, this random encounter with the edge of a diffusing patch leading to quick motion to its nutrient rich center is much more frequent than random swimming leading a cell by chance to the center of a patch. For example, let's consider again phytoplankton cells of

radius 25 μm at a cell density of $10^3$ cells/mL surrounded by chemotactic bacteria with random swimming diffusivity $D_b = 10^{-9}$ $m^2/s$ in the absence of gradients. If we assume that these bacteria can detect the edge of a phycosphere at a distance ~ 250 μm – so 10 times cell radius – away from an exudating phytoplankton cell, the average number of phycospheres encountered by random motility will be 10 times more than encounters with the phytoplankton cells themselves. Using the diffusive encounter rate estimate presented above, we can indeed estimate that a chemotactic bacterium will encounter on average 250 phycospheres per day. Each random encounter with the edge of a phycosphere can lead afterwards to chemotactic behavior to reach the phytoplankton cell. Moreover, chemotactic bacteria will be better able to retain position in a patch that they have encountered without dispersing away as would bacteria that swim randomly.

These simple estimates suggest that chemotaxis could significantly enhance the access to transient nutrient patches for copiotrophic bacteria, before they diffuse away, and thus promote the survival of these strains. Indeed, intense aggregations of bacterial cells at the microscopic scale in seawater have been observed, and it has been proposed that they arise from chemotaxis to microscale pulses of nutrients (Blackburn et al., 1998). Video microscopy observations have revealed a fast and strong chemotactic response of the marine bacterium *Pseudoalteromonas haloplanktis* to nutrient pulses, resulting in up to 87% increase in potential nutrient uptake of the population (Stocker et al., 2008). While earlier theoretical studies of these behaviors predicted only modest gains from chemotaxis (Jackson, 1987; Mitchell et al., 1985), they were based, in the absence of specific information for marine bacteria, on the behavioral parameters of *E. coli*. Marine bacteria have since been shown to possess chemotactic abilities that can be much higher than that of *E. coli* allowing cells to efficiently exploit localized nutrient patches (Mitchell et al., 1995a, 1995b, 1996; Stocker et al., 2008; Brumley et al. 2019).

Imaging of the chemotaxis of bacteria from seawater enrichments towards lysing diatoms, combined with modeling of nutrient uptake, suggests that uptake is heterogeneous, for both chemotactic and non-motile bacterial populations alike (Smriga et al., 2016). This heterogeneity stems from the short duration of the nutrient pulses, which gives advantage to cells that were already close to the source at the time of lysis. Scaling up of these results to the typical phytoplankton concentrations in the ocean predicts that chemotactic, copiotrophic strains can outcompete non-motile, oligotrophic strains during phytoplankton blooms and bloom collapse conditions, periods characterized by abundant lysing events (Smriga et al., 2016).

Chemotaxis is also important for the exploitation of particles by bacteria, where motility and chemotaxis can be beneficial in two ways. First, by increasing the encounter rate with particles, as has been demonstrated experimentally using model particles made of agar for which colonization could be quantified (Kiørboe et al., 2002). Motile bacteria have much higher rates of colonization than non-motile bacteria with chemotaxis further enhancing encounter by a factor of 5 to 10 with respect to random motility. Similarly, mathematical modeling predicts that chemotaxis enhances encounter rates with particles by two- to five-fold for particles ranging from 200 µm to 1.5 cm diameter (Kiørboe and Jackson, 2001). This increased encounter rate could explain how motile, chemotactic species – which represent a minority of bacterial cells found in the water column – are often dominant on marine particles (Fontanez et al., 2015; Ganesh et al., 2014; Guidi et al., 2016; Lambert et al., 2019; Lauro and Bartlett, 2008). Second, chemotactic bacteria can exploit the plume of nutrient leaking out of particles as they sink (Fig. 3). Assuming optimal chemotactic behavior, this use of marine snow plumes by chemotactic bacteria increases the growth rate of free-living bacteria by 2-fold for large particles (1.5 cm radius) and by 20-fold for small particles (200 µm radius) (Kiørboe and Jackson, 2001). Based on established particle size spectra in the ocean, this suggests that chemotactic bacteria would achieve a growth rate 10 times that of a non-chemotactic motile population. These predictions are supported by observations of strong bacterial accumulation within DOM plumes created in a microfluidic device, resulting in a predicted 4-fold nutrient gain of chemotactic bacteria compared to non-motile ones (Stocker et al., 2008). Together, results from these modeling and experimental studies indicate that motility and chemotaxis can greatly enhance the ability of marine bacteria to use particles and their plumes as resources.

Finally, recent work has started to reveal the impact of motility and chemotaxis on bacteria population diversity (Gude et al., 2020) and fitness (Cremer et al., 2019; Liu et al., 2019). While these works used the model enteric bacterium *E. coli* growing in soft agar plates, their findings have potential implications for the marine environment. Indeed, chemotaxis could provide a fitness advantage by driving population colonization of unexplored substrates ahead of complete nutrient depletion and starvation, as established by observing *E. coli* colony expansion on soft-agar plates (Cremer et al., 2019). This ability to colonize new resource islands could play a role in particles or sediments. Similarly, motility can promote bacterial diversity on a structured patch of resources, allowing coexistence between slow-growing motile strains and fast-growing non-motile populations (Gude et al., 2020). Indeed, while motility and chemotaxis provide fitness benefits in terms of access to nutrients, these traits are costly behaviors. It has recently been suggested that *E. coli* invests in motility and chemotactic behavior in proportion to the fitness benefit obtained by chemotaxis (Ni et al., 2020), thus demonstrating the delicate optimization of this behavior.

## 3. Sources and nature of microscale gradients in the ocean

In the ocean, the chemical seascape that bacteria experience is highly heterogeneous, characterized by vast expanses of extremely dilute background seawater punctuated by rich hotspots of dissolved and particulate nutrient resources. These chemical microenvironments are likely to be tremendously important for the growth, abundance, and diversity of bacteria (especially copiotrophs), and are derived from a diverse assortment of ecological processes, such as digestion, exudation, lysis, and excretion by the numerous members of the microbial community, but also from the diverse macroorganisms inhabiting the water column. Here we review the multiple sources of chemical gradients in the ocean that form important nutrient hotspots for heterotrophic bacteria (Fig. 5).

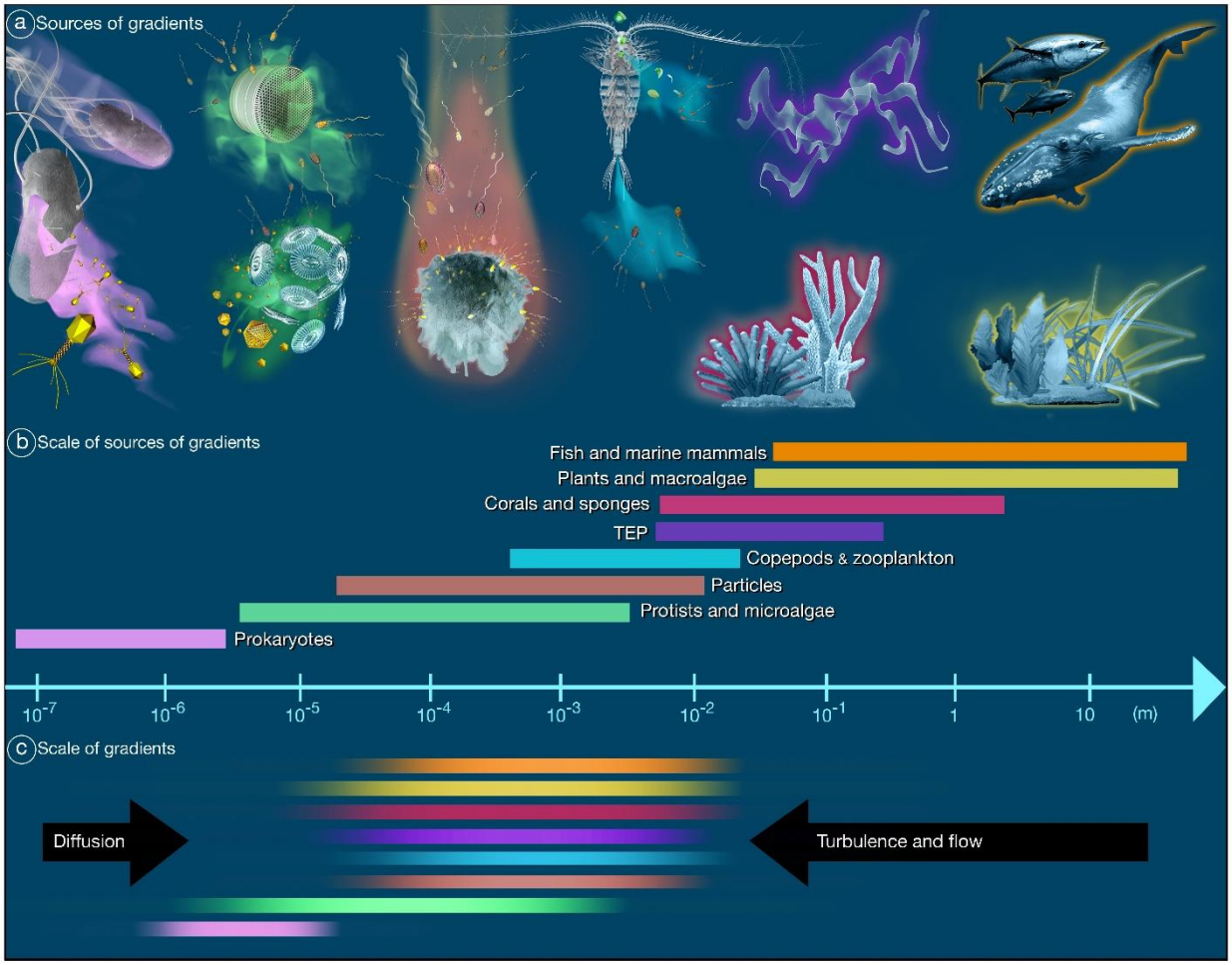


**Figure 5.** Sources of gradients in marine environments and their size ranges. (**a**) Sources of gradients. From left to right: bacterial lysis due to viral infection; phycosphere and phytoplankton lysis; sinking

particle; zooplankton excretion and sloppy feeding; transparent exopolymeric polymers (TEPs); benthic organisms such as corals and sponges; fishes and marine mammals; marine plants and macroalgae. (**b**) The scale of the sources of gradients, spanning eight orders of magnitude. (**c**) The scale of the gradients themselves, spanning four orders of magnitude. The scale of a gradient depends on the initial size of a resource patch, modulated by two processes, diffusion and turbulence/flow (as presented in section 2).

## 3.1 The phycosphere

Phytoplankton cells can release up to 50% of the carbon that they fix through photosynthesis into the surrounding seawater (Thornton, 2014), either in the form of dissolved organic molecules such as carbohydrates (monosaccharides, oligosaccharides and polysaccharides), nitrogenous compounds (amino acids, polypeptides, and proteins), fatty acids, and organic acids (glycolate, tricarboxylic acids, hydroxamate and vitamins), or as matrices made of complex polysaccharides and lipids (Aaronson, 1978; Fogg, 1977; Fossing et al., 1995; Hellebust, 1965; Jenkinson et al., 2015; Jones and Cannon, 1986; Lancelot, 1984). The exuded DOM is broadly representative of the molecular composition of phytoplankton cells, which contain approximately 25–50% proteins, 5–50% polysaccharides, 5–20% lipids, 3–20% pigments, and 20% nucleic acids (Emerson and Hedges, 2008). The monosaccharide composition of the surface ocean is similar to phytoplankton exudates, suggesting that phytoplankton is a significant source of carbohydrates in the ocean (Aluwihare et al., 1997; Biersmith and Benner, 1998).

The phycosphere is the microenvironment directly surrounding phytoplankton cells that is characterized by locally elevated concentrations of organic matter arising from the exudation of photosynthates by the phytoplankton (Bell and Mitchell, 1972; Cirri and Pohnert, 2019; Seymour et al., 2017; Smriga et al., 2016). It is considered as the aquatic analog of the rhizosphere in soil ecosystems (Philippot et al., 2013; Trolldenier, 1987) and has direct implications for nutrient fluxes to and from algal cells (Amin et al., 2012; Seymour et al., 2017). Bell and Mitchell (1972) coined the term ‘phycosphere’ based on a series of experiments where they demonstrated that filtrates from lysed phytoplankton cultures elicited significant chemotaxis, and that the release of dissolved organic matter by phytoplankton cultures contributes to the structure of their bacterial communities (Bell et al., 1974).

The phycosphere extends to a distance of a few cell diameters (Azam and Ammerman, 1984; Bell and Mitchell, 1972) and, hence, displays a large variation in sizes across species which parallels the two orders of magnitude variation in size among phytoplankton taxa (Fig 1f, Fig. 5). Furthermore, the size of the phycosphere will vary depending on phytoplankton growth and exudation rate, as well as the

diffusivity of the exuded compounds and their background concentration in bulk water (Seymour et al., 2017). For example, older cells tend to release high molecular weight DOM by secretion or cell lysis (Buchan et al., 2014; Passow, 2002), and the diverse sizes and lability of these molecules directly impact the physical characteristics of the phycosphere as well as the metabolism of surrounding bacteria. Phycospheres are also present around phytoplankton cells in motion. The chemical plume left in the wake of swimming or sinking phytoplankton cells offers a rich nutrient microenvironment that is exploitable by chemotactic bacteria (Barbara and Mitchell, 2003; Jackson, 1987, 1989).

## 3.2 Zooplankton excretion and sloppy feeding

Zooplankton ingestion, digestion, excretion, and exudation of dissolved organic carbon also contribute to the patchiness of the microscale seascape (Möller et al., 2012; Stocker and Seymour, 2012; Tang, 2005), which can also impact the growth of bacteria and phytoplankton (Birtel and Matthews, 2016; Goldman et al., 1979; Jackson, 1980; Lehman and Scavia, 1982a, 1982b). For example, zooplankton cells release organic nutrients into the water column through a process called "sloppy feeding" in which they consume their prey only partially (Blackburn et al., 1997; Lampert, 1978) and the remains therefore form a nutrient hotspot available to bacteria (Fig. 5) (Möller et al., 2012; Møller, 2005; Peduzzi and Herndl, 1992; Saba et al., 2011).

Zooplankton excretion events increase the concentrations of organic and inorganic substrates in the surrounding water (Lampert, 1978; Peduzzi and Herndl, 1992). Quantification of zooplankton-mediated DOM release has shown that *Daphnia pulex* and *Calanus hyperboreus* release up to 20% of ingested algal-derived carbon (Lampert, 1978; Copping and Lorenzen, 1980). While the size and composition of the chemical patch created by zooplankton emission will vary based on the identity of the organism releasing it, excretion events by zooplankton have been modeled as ~100 μm wide pulses of inorganic substrates such as ammonium with initial concentrations in the range 0.2–5 μM (Jackson, 1980; McCarthy and Goldman, 1979).

Copepod activity may also play a key role in providing organic substrates for bacterial growth. It was recently revealed that copepods potentially benefit from influencing the composition of microbial communities by attracting and "farming" specific bacterial species in their "zoosphere" (Shoemaker et al., 2019). Indeed, copepods may attract and support the growth of bacterial species of *Vibrionaceae*, *Oceanospirillales*, and *Rhodobacteraceae* in waters surrounding them but also appear to support the

555 growth of specific groups of bacteria in or on the copepod body, particularly *Flavobacteriaceae* and
556 *Pseudoalteromonadaceae* (Shoemaker et al., 2019).
557
558 ## 3.3 Cell lysis events
559
560 Viruses also contribute to the formation of microscale chemical gradients in the water column (Blackburn
561 et al., 1998; Ma et al., 2018; Moran et al., 2016; Riemann and Middelboe, 2002). Viral infection of
562 phytoplankton, bacterioplankton, protozoa, and other microorganisms can result in cell lysis (Middelboe,
563 2000; Riemann and Middelboe, 2002; Suttle, 1994; Suttle and Chan, 1994), whereby the host cell's
564 internal content is discharged into the water column (Fig. 5). It has been estimated that 20–50% of all
565 microbial biomass is killed daily by viruses at a rate of $10^{23}$ lysis events per second, introducing each year
566 as much as 3 Gt of carbon (Suttle, 2007) into the organic carbon pool of the ocean (45-50 Gt) (Granum,
567 2002; Granum et al., 2002).
568
569 As the internal content of a microbial cell can contain concentrations of organic compounds that are six
570 orders of magnitude higher than the bulk seawater (Flynn et al., 2008), nutrient-rich micropatches will be
571 suddenly created upon lysis (Fig. 1a-c, Fig. 5), and can persist for several minutes (Stocker and Seymour,
572 2012). Virus-infected cultures of the phytoplankton *Micromonas pusilla* release dissolved organic carbon
573 (DOC) enriched in peptides 4.5 times faster than non-infected cultures, resulting in local enrichment of
574 seawater (Lønborg et al., 2013). Studies with laboratory-based virus–host systems have shown that lysis
575 can alter the composition of DOM as well as its concentration (Middelboe and Jørgensen, 2006;
576 Weinbauer and Peduzzi, 1995). In addition, the DOM released from virally infected cells is enriched in
577 nitrogen, amino acids, and cell wall compounds, relative to the metabolites of non-infected cells (Ankrah
578 et al., 2014; Middelboe and Jørgensen, 2006). Estimates have also revealed a stochiometric mismatch
579 between phages and their bacterial hosts with the former being enriched in phosphorus (Jover et al.,
580 2014), and a subsequent modelling approach predicted that most of the phosphorus and a large fraction of
581 the iron contained in bacterial cells might in fact be sequestered in phage particles during an infection
582 (Bonnain et al., 2016). These studies have important implications for the composition and bioavailability
583 of bacterial lysates.
584
585 ## 3.4 Particles
586
587 Suspended and sinking particles provide a rich source of organic and inorganic nutrients for heterotrophic
588 bacteria (Fig. 3, Fig. 5). Concentrations of substrates associated with particles can exceed those present in

the bulk seawater by more than two orders of magnitude (Alldredge and Gotschalk, 1990). Particle dimensions range from sub-micrometer-sized colloids (Isao et al., 1990) to millimeter-sized aggregates called "marine snow" (Alldredge and Silver, 1988), which are mostly made of coagulated dead phytoplankton cells (Alldredge and Silver, 1988; Jackson, 1990; Simon et al., 2002), zooplankton fecal pellets (Jacobsen and Azam, 1984), aggregated microbial cells, and extracellular polymers (Passow, 2002).

Marine snow and other particles represent key resource hotspots prone to colonization by heterotrophic bacteria (Kiørboe et al., 2002; Ploug and Grossart, 2000; Simon et al., 2002). These microorganisms use surface-bound enzymes, including proteases, lipases, chitinases, and phosphatases to dissolve particulate organic matter (POM) contained in the aggregates through rapid hydrolysis (Smith et al., 1992). This process interrupts carbon export, converting POM into DOM, which can subsequently remain in the upper ocean. There is rapid turnover (0.2–2.1 days) of particulate amino acids into the dissolved phase with bacteria producing DOM much faster than they can use it (Smith et al., 1992). Consequently, the resources made available by this hydrolysis go beyond the particle-attached community because a substantial fraction of the solubilized organic matter leaks into the surrounding water where it becomes available to free-living bacteria (Alldredge and Cohen, 1987; Kiørboe and Jackson, 2001; Long and Azam, 2001; Stocker et al., 2008). This DOM forms a comet-like plume in the wake of particles as they sink (Fig. 3, Fig. 5) (Grossart and Simon, 1998; Kiørboe et al., 2001; Smith et al., 1992; Ya et al., 1998) and it has been predicted that free-living bacteria can exploit the DOM plume to support growth rates that are up to 10 times higher than would be possible in the surrounding seawater (Kiørboe and Jackson, 2001).

The community composition on particles is taxonomically distinct from free-living bacterial communities (DeLong et al., 1993), likely as a result of the selective pressure involved in the colonization and degradation of these nutrient hotspots. The use of synthetic polysaccharide particles has enabled to unravel the complexity of the microbial interactions occurring within these nutrient hotspots. Bacterial communities attached to these particles undergo rapid and reproducible successions under laboratory conditions (Datta et al., 2016). Indeed, a shift occurs from early colonizers that are motile and degrade organic matter derived from the particles to secondary consumers that fully rely on the metabolic byproducts of the primary degraders and who cannot directly consume particle-derived carbon (Datta et al., 2016). In addition, metabolic interactions alongside the spatial organization of bacteria on these particles influence the uptake of particle-derived carbon (Ebrahimi et al., 2019).

## 3.5 Transparent exopolymer particles

The traditional view of the microbial seascape as a simple dichotomy between particulate matter and dissolved organic matter may be an over-simplification. Diverse compounds known as TEP (transparent exopolymer particles), including organic gels, colloids and matrices (Alldredge et al., 1993; Long and Azam, 2001), bridge the two ends of the spectrum of the resource seascape, which has been described instead as an "organic matter continuum" (Azam, 1998). Many microbial compounds, such as the large quantities of exopolymeric material released by diatoms and bacteria (Alldredge et al., 1993; Gärdes et al., 2011; Jenkinson et al., 2015; Long and Azam, 2001), are characteristic of the transition phase between particulate and dissolved organic matter. The sticky nature of exopolymers promotes the aggregation of organic matter and microbes and therefore promotes carbon export from the euphotic zone to the deep ocean (Engel et al., 2004; Mari et al., 2017). However, exopolymers also facilitate the attachment of particle-degrading bacteria for which they provide an additional carbon source (Passow, 2002; Taylor and Cunliffe, 2017) (Fig. 5). For example, by using DNA stable-isotope probing, members of the *Alteromonadaceae* have been shown to assimilate $^{13}$C-TEP carbon (Taylor and Cunliffe, 2017), which is consistent with their capability to produce a suite of polysaccharide-degrading enzymes (Teeling et al., 2016).

## 3.6 Larger organisms

Chemical gradients in the water column also emanate from larger organisms such as fish and mammals (Fig. 5). As a rich source of organic molecules, the skin of fish can be colonized by numerous bacterial taxa (Sar and Rosenberg, 1987; Shotts et al., 1990), such as the mucus-colonizing community dominated by the phylum *Proteobacteria* found on the skin of Atlantic salmon (Minniti et al., 2017). Benthic organisms, such as coral, seaweed, sponges, and bivalves, represent other sources of strong chemical gradients (Fig. 5). Surprisingly, surface metabolites released by the coral colonies can form concentration gradients extending up to 5 cm away from the coral surface (Ochsenkühn et al., 2018), a distance much greater than typical diffusion boundary layers. Corals excrete a mucus layer than can be hundreds of microns thick (Paul et al., 1986; Rohwer et al., 2001, 2002). This mucus contains organic and inorganic compounds at concentrations that are 3–4 orders of magnitude higher than the background seawater (Broadbent and Jones, 2004; Wild et al., 2004) and it has been proposed that microbial colonization of this coral surface layer plays an important role in coral-microbe interactions and even in symbioses (Blackall et al., 2015; Pogoreutz et al., 2021; Pollock et al., 2018). Marine sponges also exude chemicals and are known "microbial hotspots" because they harbor dense and diverse microbial communities, which

can account for up to 40% of a sponge's biomass (Taylor et al., 2007; Webster and Taylor, 2012; Webster and Thomas, 2016). Marine plants and algae represent another important source of chemical gradients (Haas and Wild, 2010; Moriarty et al., 1986). For instance, the benthic alga *Halimeda opuntia* releases a large amount of carbohydrates and proteins into the surrounding seawater (up to 2 mg $m^{-2}$ $h^{-1}$) sustaining the growth of bacteria in their vicinity (Haas and Wild, 2010).

## 3.7 The sediment–water interface

The solid–liquid interface at the surface of marine sediments is a site of intense microbial activity due to its high concentration of organic material, which originates from deposited marine particulate organic matter that sank from the surface waters (Burdige and Komada, 2015; Cai et al., 2019; Rossel et al., 2016; Zhang et al., 2018).

The concentration of dissolved organic carbon present in coastal sediments can be more than an order of magnitude higher than in the water directly above this interface (Burdige and Gardner, 1998) indicating net production of DOM in sediments resulting from degradation processes (Burdige and Komada, 2015). Experiments have demonstrated that in certain cases bacteria and archaea can sustain these gradients on timescales of hours to tens of hours in response to substrate addition by producing extracellular enzymes triggering extremely rapid hydrolysis of high molecular weight organic matter to low molecular weight DOM (Arnosti, 2004; Burdige and Komada, 2015), resulting in the production of small organic molecules and inorganic compounds ($H_2S$, $NH_4^+$, $Fe^{2+}$) (Jørgensen and Revsbech, 1983; Ramsing et al., 1993; Schulz and Jørgensen, 2001).

The active biological degradation of organic matter in sediments results in steep vertical gradients of nutrients and counter-gradients of oxygen or hydrogen sulfide (Jørgensen and Revsbech, 1983; Jørgensen et al., 2019), which generates chemical habitats that are remarkably different from the pelagic environment (Schulz and Jørgensen, 2001). Indeed, the water–sediment interface is best described as a one-dimensional collection of chemical gradients that are more stable through time than the complex three-dimensional and often short-lived chemical gradients present in the water column (Fig. 5). The surface sediments are often dominated by sulfur oxidizers, such as *Thiovulum majus*, one of the fastest swimming bacteria recorded (swimming at up to 600 µm $s^{-1}$; Jørgensen and Revsbech, 1983), which uses chemotaxis to form dense aggregations in the narrow region where optimal concentrations of oxygen and hydrogen sulfide co-exist (Petroff and Libchaber, 2014; Petroff et al., 2015). Furthermore, the large size of *T. majus* of up to 25 µm in diameter makes this bacterium immune to Brownian rotational diffusion

and therefore considerably more effective at controlling its swimming direction than the small bacteria of the water column (Fenchel, 1994).

### 3.8 Molecular diversity of chemoattractants

Oceanic DOM is extremely diverse in its chemical composition as might be expected from the wide range of organisms contributing to this pool, and recent estimates revealed that hundreds of thousands of different organic molecules might be present (Amon et al., 2001; Kim et al., 2003; Kujawinski et al., 2016) amounting to almost as much carbon as $CO_2$ in the atmosphere (Moran et al., 2016). Recent advances in DNA sequencing (DeLong and Karl, 2005), mass spectrometry (Hartmann et al., 2017) and bioinformatics (Dührkop et al., 2015; Watrous et al., 2012) have enabled a giant step forwards in the identification and characterization of the key chemical currencies in the ocean, each of which has the potential to induce behavioral responses, generate interactions among organisms, and sustain the growth of specific marine bacteria. However, not all compounds have the same nutritive value to bacteria, as foraging strategies and chemotactic preferences are strain-specific (Amin et al., 2012; Seymour et al., 2010a).

DOM can be categorized along a gradient of reactivity, from labile to semi-labile to refractory, based on persistence in the water column (Hansell, 2013). Compounds referred to as labile DOM are typically consumed within hours to days of production, although their half-lives have been estimated to be in the order of minutes at picomolar concentrations (Azam, 1998), which complicates an accurate quantification of their abundance and lifetime in the water column. For example, the bulk concentrations of amino acids or sugars are usually just above the detection limit of most analytical instruments (a few nM per liter) (Kaiser and Benner, 2012; Mopper et al., 1992). Yet, they represent a large proportion of the DOM taken up by bacteria (Hollibaugh and Azam, 1983) and their rapid turnover is likely to keep their concentrations low. Most of the labile DOM consists of highly diverse compounds derived from phytoplankton primary production and is dominated by proteins and carbohydrates (Ferguson and Sunda, 1984; Hodson et al., 1981; Vorobev et al., 2018) but also contains mono- and dicarboxylic acids (Gifford et al., 2013; Poretsky et al., 2010), glycerols and fatty acids (Gifford et al., 2013; McCarren et al., 2010), single-carbon compounds such as methanol (Gifford et al., 2013; Lidbury et al., 2014; McCarren et al., 2010), sulfonates (Durham et al., 2015), as well as the nitrogen-containing metabolites taurine, choline, polyamines, and ectoine (Gifford et al., 2013; Lidbury et al., 2014; Liu et al., 2015).

Compounds referred to as semi-labile are less reactive and persist longer in the surface ocean, from weeks to years (Hansell, 2013), but might ultimately be exported to depth and buried in marine sediments for millennia (Hansell and Carlson, 1998). Examples of semi-labile DOM include large polysaccharides and dissolved combined neutral sugars (Panagiotopoulos et al., 2019). Finally, the term refractory DOM is used to characterize the least reactive and most persistent fraction potentially stored in ocean basins for millennia (Follett et al., 2014; Williams and Druffel, 1987). These refractory molecules might account for 95% of the dissolved organic carbon found in the ocean (~624 Gt of C) and contribute to long-term carbon storage (Jiao et al., 2010; Ogawa et al., 2001). Despite its ubiquitous presence in the ocean, the pool of refractory DOM is poorly characterized and the role that specific microbial species play in producing or partially degrading these molecules has not been elucidated (Osterholz et al., 2015). In addition, the distribution of specific molecules between these three categories is not well established largely due to the vast chemical diversity of the DOM pool. Our understanding of the 'chemical preferences' of marine bacteria in term of chemotaxis and substrate utilization is still restricted to a few molecules and species.

# 4. Motility and chemotaxis as microbial adaptations to microscale heterogeneity in the ocean

The previous section described the vast array of nutrient gradients that prokaryotic cells may encounter in the water column. Homing in on these gradients using motility and chemotaxis can therefore be highly beneficial for bacteria and archaea. Cells are propelled by phosphorylation-triggered rotating flagella (Wadhams and Armitage, 2004) and can reorient themselves towards food patches using sensitive sensing mechanisms (Lux and Shi, 2004). While hotspots can be abundant, during a bloom of phytoplankton for example, many regions of the ocean are characterized by low background nutrients, which result in lower biomass and sparser number of available hotspots. This implies that motility and chemotaxis in the marine environment need to be adapted to explore wide areas and efficiently sense small increase in chemical concentration above background levels. Indeed, many marine bacteria possess motility adaptations including fast swimming and specific reorientation strategies that differentiate them from classic model systems such as *Escherichia coli* and are more suited to the harsh nutrient conditions of the ocean.

## 4.1 The molecular machinery of chemotaxis

The molecular machinery underpinning chemotactic behaviors has been extensively studied in *E. coli*. Upon detection of the chemical gradient of a chemoeffector (a chemical that attracts or repels cells), the

bacteria's sensory system (Fig. 6) triggers a change in the swimming pattern to bias movement toward the higher concentration of a chemoattractant or toward lower concentration of a chemorepellent. The sensory system of *E. coli* is sensitive enough to detect changes in receptor occupancy of a few molecules against background concentrations and can detect variation over five orders of magnitude (Kim et al., 2001; Sourjik and Berg, 2002a).

When *E. coli*'s chemotactic sensory machinery encounters a steep gradient of a chemoattractant, the cell's run-time increases from 1 s to over 10 s. Chemoeffectors binding to the cell's receptors induce an excitatory pathway that results in the modulation of the flagellum's motor (Segall et al., 1982; Sourjik and Berg, 2002b). Upon encounter of an attractant, the flagella move in a counterclockwise motion; conversely, flagella move clockwise upon encounter of a repellent or a lower concentration of an attractant (Berg and Tedesco, 1975) inducing a change of orientation. The time interval between the onset of the stimulus and the clockwise-to-counter-clockwise transition is a linear function of the change in receptor occupancy (Berg and Tedesco, 1975). Despite variation in the number and location of flagella among bacterial strains, all chemosensory pathways of chemotaxis rely on modulation of the rotation of the flagellar motor (Wadhams and Armitage, 2004).

Gradient sensing is accomplished by comparing the cell's receptor occupancy through time. *E. coli* makes short-term comparisons up to 4 s in the past where the most recent 1 s is given a positive weighting and the previous 3 s a negative weighting (Segall et al., 1986). The cell responds according to the overall weighted sum (Segall et al., 1986), which leads to a chemical "memory" (Berg and Tedesco, 1975). At the molecular level, the signaling pathway involved in chemotaxis relies on a histidine–aspartate phosphorelay pathway and is probably one of the best-described processes in biology. The pathway is composed of transmembrane chemoreceptors (methyl-accepting chemotaxis proteins, MCPs) that detect binding chemoeffectors (Fig. 6a). Chemotactic bacteria possess on average 14 different MCPs (Lacal et al., 2010); however, this number can vary greatly at the strain level from as few as one to as many as 90 (Alexandre et al., 2004; Salah Ud-Din and Roujeinikova, 2017). With the help of the adaptor protein CheW, the MCPs are connected to the histidine protein kinase chemotaxis protein CheA, which can sense chemical inputs through the MCPs. Two diffusible response regulators, CheY and CheB, then compete for binding to CheA (Fig. 6a). The phosphorylated motor-binding protein CheY-P controls flagellar motor rotation by binding to the switch protein FliM, which leads to a reversal in the direction of the motor rotation (Wadhams and Armitage, 2004) whereas the methylesterase CheB controls adaptation of the MCPs (Anand et al., 1998; Hess et al., 1988). An additional molecule, CheZ, is required to increase the rate of dephosphorylation of CheY-P to induce a time-efficient signal termination (McEvoy et al., 1999).

Consequently, an extracellular decrease of chemoattractant concentration leads to a decreased rate of binding to the MCPs, which induces the trans-autophosphorylation of CheA and an increased amount of CheY-P in the cytoplasm through its direct phosphorylation (Fig. 6a). CheY–P then binds to the flagellar motor and stimulates a switch in rotation to a clockwise motion (Fig. 6a, b) resulting in the bacterium tumbling and hence changing swimming direction. The concentration of CheY–P is then decreased by the phosphatase CheZ. Simultaneously, the methylesterase activity of CheB is increased by phosphorylation from CheA–P, so that CheB-P induces demethylation of the MCPs thereby limiting the rate of CheA autophosphorylation. Consequently, the rate of switching in rotation then returns to the levels before stimulus and the cell is primed to react to any additional increase or decrease in chemoeffectors on the receptors. In the opposite case of an increase of chemoattractant concentration binding to the MCPs, the autophosphorylation of CheA is inhibited resulting in a reduction of the cytoplasmic CheY-P concentration and hence a decrease in the frequency of motor switching. Consequently, the cell swims longer in the same direction before tumbling. Additionally, the phosphorylation and activity of CheB are decreased so that the constitutive levels of the methyltransferase CheR then lead to a higher level of methylation of the MCPs. The MCPs are thus more capable of causing CheA autophosphorylation so that its rate returns to pre-stimulus levels and brings the bacterium back to a normal frequency of tumbling.

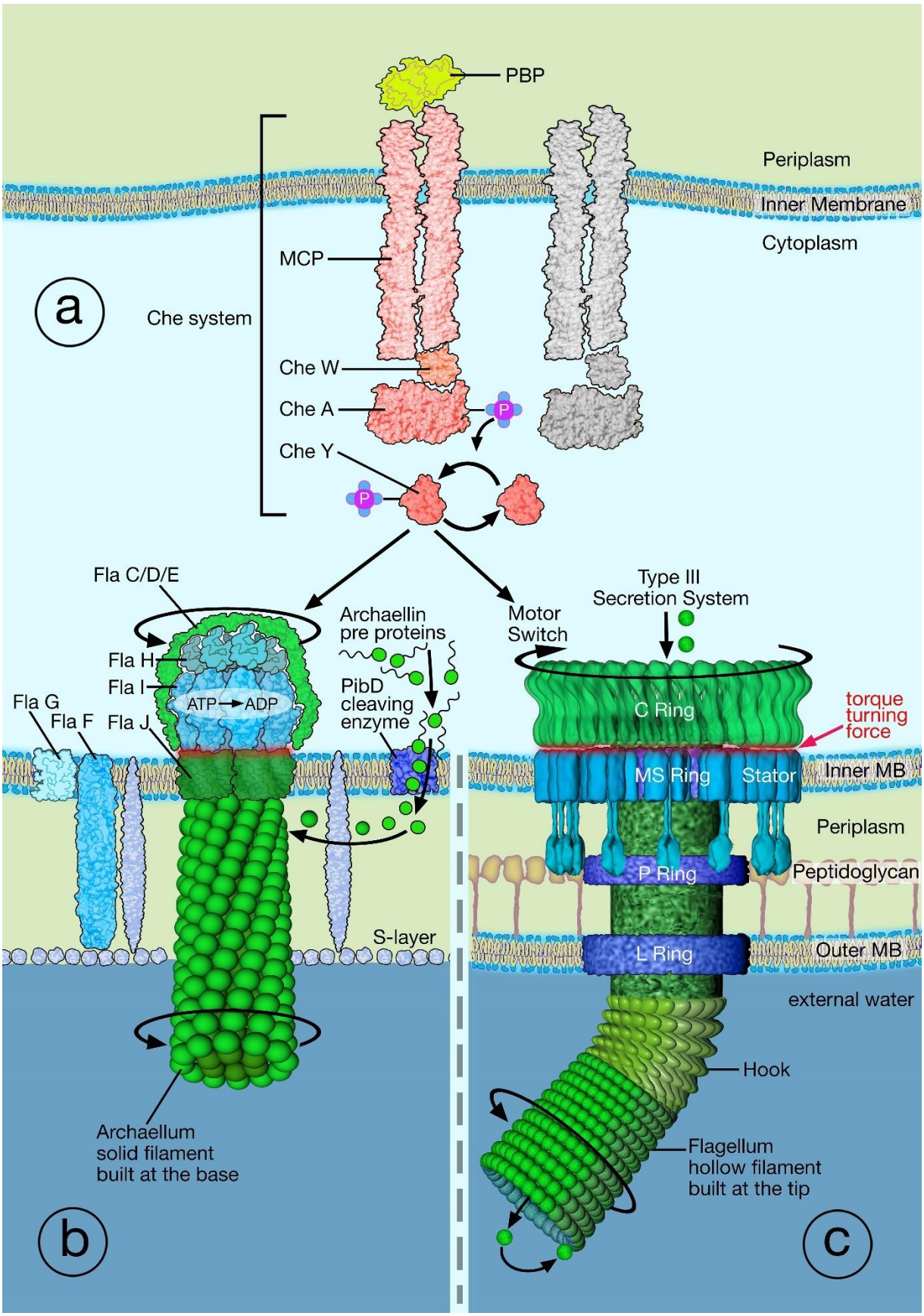
PBP
Periplasm
Inner Membrane
Cytoplasm
MCP
a
Che system
Che W
Che A
P
Che Y
P
Fla C/D/E
Archaellin
pre proteins
Motor
Switch
Type III
Secretion System
Fla H
Fla I
ATP → ADP
PibD
cleaving
enzyme
Fla G
Fla F
Fla J
C Ring
torque
turning
force
MS Ring
Stator
Inner MB
Periplasm
P Ring
Peptidoglycan
S-layer
L Ring
Outer MB
external water
Hook
Archaellum
solid filament
built at the base
Flagellum
hollow filament
built at the tip
b
c

809

**Figure 6.** Molecular machinery of motility and chemotaxis in bacteria and archaea. (**a**) Representation of the chemotaxis sensing apparatus of both organisms showing the transduction of a signal (Periplasm Binding Protein PBP) from the receptors (Methyl-accepting Chemotaxis Protein MCPs) to CheW and to the phosphorylation of CheA. CheA phosphorylates CheY, and CheY-P then diffuses to the flagellum base. (**b**) In archaea, a rotation occurs when CheY binds to adaptor protein CheF (Schlesner et al., 2009) to navigate to the motor switch, constituted of the archaeal-specific proteins FlaC/D/E. FlaH, FlaI and FlaJ form a core motor platform. FlaF and FlaG provide a rigid structure between the S-layer and the rotating components of the motor (FlaJ) (Banerjee et al., 2015; Tsai et al., 2020). PibD, a prepilin peptidase, cleaves the N-terminus of the archaellins before assembly on the growing structure. (**c**) In bacteria, phosphorylated CheY binds to the switch complex and induces a change of rotation.

## 4.2 The roles of chemotaxis

Chemoattractants play at least two ecological roles. Most often they serve as high-quality bacterial substrates that bacteria can readily use to sustain growth (Cremer et al., 2019; Stocker et al., 2008). However, some microbial chemoattractants do not act as substrates but instead, serve only as signaling compounds, directing bacteria to ecologically advantageous microenvironments without being consumed (Seymour et al., 2017; Yang et al., 2015). For example, *Vibrio furnissii*, a chitin degrader, uses the water-soluble products of chitin hydrolysis as a cue to locate chitin (Bassler et al., 1991) and *V. coralliilyticus* uses dimethylsulfoniopropionate (DMSP) as a cue to locate its coral host (Garren et al., 2014) in both cases without the chemoattractant being metabolized. Chemoattractants as signaling molecules have also been reported in *B. subtilis* (Yang et al., 2015). In a comparison of the chemotactic response of *E. coli* and *B. subtilis* to a set of amino acids, the chemotactic response of the former was correlated with amino acid use, while no such correlation was found with the latter (Yang et al., 2015). This suggests that amino acids did not induce chemotaxis in *B. subtilis* because of their nutritional value but instead served as environmental cues.

## 4.3 Mechanics of motility

At the molecular level, bacterial motility is achieved through the use of one or more helical flagella, which are used to propel cells and thus to explore and eventually exploit their environment (Stocker, 2012). By utilizing a proton or sodium gradient (Berg, 2008) molecular motors rotate each flagellum in a corkscrew motion and thereby propel the bacterium forward. These microscale movements are also not

benefiting from inertia meaning that once the bacterium's flagella stop moving the cell will immediately stop its forward motion (within a distance of less than one hydrogen atom) (Purcell, 1977).

Bacterial motility has been well studied in *E. coli* (Berg, 1993, 2000, 2008) that possesses 4–8 proton-powered flagella (Berg, 2008). Its motility pattern has been described as a "run and tumble" random walk (Berg, 1993). Runs, periods of nearly straight-line swimming lasting 1–4 s, are generated by counterclockwise movement of the flagella that coalesces them into a bundle that propels the cell at 10–30 μm/s. Tumbles occur when at least one motor reverses direction and disrupts the flagella bundle, which triggers a very short (~0.1 s) random reorientation biased in the direction of the previous run (Berg, 2008; Berg and Brown, 1972).

Similarly to bacteria, archaea also have the ability to produce a propulsive force and direct their movement toward nutrient-rich hotspots in the ocean with the help of a flagellum-like filament, the archaellum (Fig. 6c) (Alam et al., 1984; Albers and Jarrell, 2018; Jarrell and Albers, 2012; Khan and Scholey, 2018; Silverman and Simon, 1974). Although this archaea-specific system has a similar function to the bacterial flagellum its molecular organization is radically different (Jarrell and Albers, 2012; Thomas et al., 2001). Indeed, the archaellum's structure consists of only 8–13 proteins none of which share homologies with the 30 flagellar structural proteins called flagellins (Chaban et al., 2007; Lassak et al., 2012; Macnab, 2003). The archaellum's assembly mechanism is analogous to that of bacterial type IV pili (Jarrell and Albers, 2012; Jarrell et al., 1996). Additionally, whereas bacterial flagella are actuated by proton or sodium-driving forces, the archaellum's rotation is driven by ATP hydrolysis (Hirota and Imae, 1983; Kinosita et al., 2016; Manson et al., 1977; Streif et al., 2008).

## 4.4 Abundance of motile prokaryotes

Although the most abundant taxa of marine bacteria are non-motile such as *Pelagibacter ubique* (Morris et al., 2002) and *Prochlorococcus* (Liu et al., 1997; Moore et al., 1998) increasing evidence suggests that the fraction of marine microorganisms capable of motility can be important. Microscopy cell counts suggest that motile prokaryotes represent on average 10% of the total of bacterial and archaeal cells in coastal seawater samples but can increase to 80% over a short period of time (~12 h) upon enrichment with organic substrates (Mitchell et al., 1995a, 1995b). Without enrichment the motile fraction of bacteria ranges between 5% and 70% (Fenchel, 2001; Grossart et al., 2001). This large range has been attributed to variation with depth, with seasonal and daily cycles, and the amounts of dissolved and particulate organic matter in the water column associated with events such as phytoplankton blooms (Buchan et al.,

2014; Engel et al., 2011; Grossart et al., 2001). These surveys also indicate that motility appears to be widespread in eutrophic coastal regions and in productive surface waters both of which are characterized by a high level of patchiness in the resource seascape. However, most approaches quantifying motility in bacterial communities are more than 20 years old and new methods enabling high-throughput quantification of motility in a variety of marine environments are needed.

## 4.5 Swimming speed

Marine bacteria are typically much faster than the enteric bacterial models. This difference comes in part from the molecular motors they use, which are powered by sodium gradients across the cytoplasmic membrane instead of the proton gradients used by *E. coli* (Li et al., 2011; Magariyama et al., 1994). For example, the marine bacterium *Vibrio alginolyticus* swims faster with increasing sodium concentrations in surrounding bulk water (Muramoto et al., 1995; Son et al., 2013), and its flagellum rotate about 4–6 times faster than those of *E. coli* (Yorimitsu and Homma, 2001). The swimming speed measured for marine isolates or marine bacteria in natural communities ranges from 45 to 230 µm/s (Grossart et al., 2001; Hütz et al., 2011; Johansen et al., 2002; Mitchell et al., 1995a, 1995b; Muramoto et al., 1995; Seymour et al., 2010b; Shigematsu et al., 1995; Stocker et al., 2008; Xie et al., 2011) (Table 1). A survey revealed that most of the average swimming speeds of 84 marine isolates fell in the range 25–35 µm/s (Table 1) (Johansen et al., 2002). However, some species consistently swim faster than this average, such as *Pseudoalteromonas haloplanktis* (68–80 µm/s) (Seymour et al., 2010b; Stocker et al., 2008), *Thalassospira* (62 µm/s) (Hütz et al., 2011), and *Vibrio alginolyticus* (45–116 µm/s) (Muramoto et al., 1995; Xie et al., 2011) (Table 1). *Thiovolum majus* and *Ovobacter propellens*, residents of the sediment–water interface, are the fastest bacteria recorded so far, swimming at a striking 600 µm/s (Fenchel, 1994) and 1000 µm/s (Fenchel and Thar, 2004), respectively.

Compared to marine bacteria few studies exist on archaeal motility. The swimming mechanism of the rod-shaped *Halobacterium salinarum* is the rotation of its archaella (Alam and Oesterhelt, 1984; Alam et al., 1984). For these archaea a simple back and forth movement was observed and the swimming speed of the cells was very low (2 µm $s^{-1}$). *Haloferax* sp. and *Haloarcula* sp. both exhibit 'run and reverse' swimming patterns with low average speeds of ~2 µm $s^{-1}$ and ~2.3 µm $s^{-1}$, respectively (Thornton et al., 2020). The recent use of 3D-holographic microscopy and computer simulations revealed that halophilic archaea's swimming direction was stabilized by their archaellum, allowing for sustained directional swimming as well as energetic costs 100-fold lower than in common bacterial model systems (Thornton et al., 2020). However, not all archaea swim slowly. Two Euryarchaeota (*Methanocaldococcus jannaschii*

and *M. villosus*) living in deep hydrothermal vents possess more than 50 polar archaella and are the fastest archaea observed so far reaching striking speeds of 400 and 500 $\mu m\ s^{-1}$, respectively (Herzog and Wirth, 2012) (Table 1).

**Table 1:** Recorded swimming speeds of bacteria and archaea.

| Bacterial/archaeal species | Environment | Speed (µm/s) | References |
|---|---|---|---|
| ***Escherichia coli*** | enteric | 10–30 | Berg, 2008; Berg and Brown, 1972 |
| ***Serratia marcescens*** | soil/enteric | 26 | Edwards et al., 2014 |
| ***Pseudomonas aeruginosa*** | ubiquitous | 51–60 | Conrad et al., 2011; Hook et al., 2019 |
| ***Bradyrhizobium diazoefficiens*** | soil | 27.5–29.8 | Quelas et al., 2016 |
| ***Pseudomonas putida*** | soil | 44–75 | Harwood et al., 1989 |
| ***Pseudomonas fluorescens*** | soil | 77–102 | Ping et al., 2013 |
| ***Vibrio splendidus*** | marine | 20 | Johansen et al., 2002 |
| ***Colwellia demingiae*** | marine | 17–27 | Johansen et al., 2002 |
| ***Agrobacterium sanguineum*** | marine | 25 | Johansen et al., 2002 |
| ***Vibrio cholerae*** | marine | 75 | Shigematsu et al., 1995 |
| ***Pseudoalteromonas haloplanktis*** | marine | 68–80 | Seymour et al., 2010b |
| ***Thalassospira* sp.** | marine | 62 | Hütz et al., 2011 |
| ***Vibrio alginolyticus*** | marine | 45–116 | Muramoto et al., 1995; Xie et al., 2011 |
| ***Methanocaldococcus jannaschii*** | marine | ~400 | (Herzog and Wirth, 2012) |
| ***Methanocaldococcus villosus*** | marine | ~500 | (Herzog and Wirth, 2012) |
| ***Thiovulum majus*** | marine | 600 | Fenchel, 1994 |
| ***Ovobacter propellens*** | marine | 1000 | Fenchel and Thar, 2004 |

## 4.6 Why do marine bacteria swim fast?

The ephemeral nature of many nutrient sources in the ocean implies that fast responses are beneficial to increase nutrient uptake. The primary parameter affecting the chemotactic response rate is the swimming speed: its importance in different ecological processes, including the colonization of particles and the

uptake of dissolved nutrients, has been determined by numerical simulations (Kiørboe and Jackson, 2001) and experiments (Stocker et al., 2008).

Fast swimming does not increase the flux of nutrients to bacteria. As the fluid flow generated by swimming decreases the thickness of the diffusion boundary layer surrounding a cell (see section 2), it can induce an increased nutrient flux to the cell leading to a higher uptake rate of resources per unit time. However, this increased uptake rate is size-dependent, and sizeable advantages are only expected for very large cells (> 10 µm), being negligeable for most marine bacteria (Guasto et al., 2012). However, the effect of Brownian motion on bacteria might be an evolutionary reason for increased swimming speeds in bacteria found in the water column. The smaller a bacterium is the more prone it is to be redirected in a random direction due to Brownian motion while swimming, thereby disrupting directional swimming and chemotaxis (Berg, 2008; Mitchell, 1991). This effect can be quantified using the rotational diffusivity $D_R = kT/(8\nu\pi\mu R^3)$ of a spherical bacterium of radius $R$, where µ is the dynamic viscosity of water, $k$ is Boltzmann's constant and $T$ is the temperature in degrees Kelvin. For a bacterium of $R$ = 0.6 µm the rotational diffusivity is 0.76 rad$^2$/s, which implies the generation of rotation of $(4D_Rt)^{1/2}$ that is 100 degrees over 1 second, which will rapidly bring a cell off course. Even though cell shape (e.g. elongation, curvature) and the presence of a flagellum provide stability to marine bacteria against reorientation (Schuech et al., 2019; Guadayol et al., 2017; Mitchell, 1991), Brownian motion effects impose a strong selective pressure for fast motility in small bacteria because faster cells will explore a longer distance before being spun off course.

## 4.7 Energetic costs and benefits of motility

The high swimming speeds of marine bacteria come with an energetic cost. Early studies based on *E. coli* described bacterial motility as inexpensive (Purcell, 1997) estimating that the costs of flagella synthesis and operation only amount to a modest ~0.1% of *E. coli*'s total energy expenditure (Macnab, 1996). However, *E. coli*'s natural environment, the animal gut, harbors nutrient concentrations 2–4 orders of magnitude higher than those found in the ocean. In addition, marine bacteria, which swim about 3 to 5 times faster than *E.coli*, will incur an energy expenditure of about 10 to 25 times greater because of the propulsive power required in the viscosity-dominated regime in which bacteria live increases with the square of the swimming speed (Taylor and Stocker, 2012). This energy demand imposes a strong selective pressure on bacterial motility in the ocean, a consideration supported by the large proportion of non-motile marine bacteria that emphasizes the tradeoffs of motility and chemotaxis in the water column.

Mathematical simulations of bacterial competition in turbulent flow provide means to estimate the fitness advantage of chemotaxis (Taylor and Stocker, 2012). Estimates of the potential gain of resources provided by chemotaxis and the energy expenditure due to swimming under realistic marine conditions suggest that if a bacterium is motile its optimal swimming speed in the pelagic environment should be ~60 µm/s (Taylor and Stocker, 2012; Watteaux et al., 2015). This theoretical value is close to the reported speeds of diverse marine bacterial taxa (Table 1) (Seymour et al., 2010b; Stocker et al., 2008). However, important parameters such as the costs of flagella and motor synthesis, production and activation of the signal transduction machinery, and ecological costs such as the effect on encounter rates with predators and viruses, have not yet been integrated in order to better estimate the cost of motility and chemotaxis.

One way that motile marine bacteria can save energy is by not swimming at a constant speed. Taylor and Stocker (2012) hypothesized that swimming speed may be adaptive and that cells might be able to regulate their speed upon encounter of chemical signals. This behavior, known as "chemokinesis", is supported by several observations. For example, *Pseudoalteromonas haloplanktis* displays a 20% increase in swimming speed when located within a patch of algal exudates (Seymour et al., 2009a). Similarly, *Vibrio coralliilyticus* swims 50% faster when exposed to the mucus of its coral host (Garren et al., 2014). Similar variation in swimming speeds over timescales of tens of seconds has been reported for natural assemblages of microorganisms under laboratory conditions (Grossart et al., 2001).

## 4.8 Swimming patterns

The fast swimming speeds of marine bacteria contribute to their high chemotactic performance but other factors also play a role. The chemotactic efficiency, $V_C/V_S$, representing the ratio between the chemotactic speed $V_C$ and the swimming speed $V_S$, is independent of the swimming speed as $V_C$ increases linearly with $V_S$ and therefore leads to a constant ratio. A perfectly directional response up the gradient excluding any random reorientation would result in a chemotactic efficiency of 1 whereas in the opposite case, a repulsion perfectly anti-directional to the gradient would result in $V_C/V_S = -1$. Between these extremes, a chemotactic efficiency of 0 characterizes purely random motion. While the chemotactic efficiency of *E. coli* typically ranges between 0.05 and 0.15 with exceptional peaks of 0.35 (Ahmed and Stocker, 2008) marine bacteria achieve a chemotactic efficiency of up to 0.5 (Seymour et al., 2010a) in line with the idea that a rapid and directional response can provide an ecological advantage in a nutrient environment characterized by ephemeral hotspots.

Chemotaxis of *E. coli* has been further compared to the marine bacterium *P. haloplanktis* when subjected to 10-min nutrient pulses in microfluidics setups revealing that the chemotactic response of *P. haloplanktis* is almost 10 times faster than that of *E.coli* (Stocker et al., 2008). In addition, *P. haloplanktis* accumulated more strongly in the high concentration regions resulting ultimately in a 64–87% increase in potential nutrient uptake of the entire population and a 10-fold increase for the fastest 20% of bacteria (Stocker et al., 2008). Modeling revealed that this chemotactic performance could not be solely attributed to higher swimming speeds (68 µm/s for *P. haloplanktis* vs. 31 µm/s for *E. coli)* but resulted also from their highly directional swimming patterns (i.e., higher $V_C/V_S$). These results highlight the importance of considering the overall swimming behavior of a bacterium, rather than only its swimming speed to fully understand the extent of its motility capacities.

This picture of motility and chemotactic performance is further completed by understanding how bacteria change direction along their course. *E. coli* uses a run-and-tumble swimming pattern: during each tumble, a cell's direction of motion is reoriented by a nearly random angle with the distribution of angles having a mean of 68° (Berg, 2008). Yet, this is only one of several swimming strategies exhibited by bacteria (Mitchell and Kogure, 2006). *Vibrios*, among other marine bacteria, swim using a single polar flagellum. This leads to a bidirectional movement, which was historically described as "run and reverse" (Johnson et al., 1992; Mitchell et al., 1996): when the flagellum rotates in one direction the cell swims forwards and when the flagellum reverses direction the cell swims backwards. This swimming pattern is marked by 180° reorientations of swimming direction, which would lead to constant back and forth swimming along the same line if Brownian rotational diffusion did not introduce randomness in the swimming directionality along each run. Run and reverse motility was historically considered as the most prevalent swimming pattern among marine bacteria (Johnson et al., 1992) and reversals have been proposed - on the basis of a mathematical model - to be more efficient than tumbles in enabling bacteria to stay close to a nutrient point source under the shear associated for example with turbulence (Luchsinger et al., 1999).

Recently, a new swimming pattern, 'run-reverse-and-flick' motility, has been identified and appears to be widespread among marine bacteria. High-resolution imaging of *V. alginolyticus* (Xie et al., 2011) showed that cells follow a strict sequence of run, reverse (180° change of direction), and 'flick', where the latter action is the previously unreported form of reorientation. Cell tracking and fluorescence labelling of the flagellum revealed that the flick, characterized by a normal distribution of reorientation angles with a mean of 90°, results from a large, whip-like deformation of the single polar flagellum. Using this hybrid motility (Stocker, 2011), *V. alginolyticus* achieves a comparable exploration of its environment to that of *E. coli* and does so without requiring multiple flagella, which in the nutrient-poor ocean would be

expensive to build. High-speed video microscopy has revealed that the flick occurs approximately 10 ms after the onset of a forward run rather than at the end of a backward run (Son et al., 2013). This timescale is faster than the time between two frames of standard cameras (33 ms), providing a potential reason for why flicks had not been detected before and why many or possibly all strains previously characterized as swimming in a "run-and-reverse" mode may actually be swimming in a 'run-reverse-and-flick' mode.

The brief forward motion before a flick provided an important clue as to the mechanism of the flick: a compressive force exerted by the forward propulsion causes a mechanical buckling instability in the flagellum's hook. To what extent an actual 'run-and-reverse' pattern is exhibited by bacteria in the ocean remains an open question but – on the grounds that the flick provides a much more effective and rapid form of reorientation than Brownian reorientation coupled with the fact that rapid navigation is critical to exploit transient microscale hotspots in the ocean – we propose that a minority if any marine bacteria swim in a run-and-reverse mode whereas we expect run-reverse-and-flick to be pervasive among marine bacteria, considering the large fraction of marine bacteria that have a single flagellum (Leifson et al., 1964). Finally, the flick could be instrumental in allowing fast bacteria to accumulate at the top of nutrient gradients. For instance, (Son et al., 2016) investigated the relationship between swimming speed, flicking motility, and high-performance chemotaxis by tracking large numbers of individual *V. alginolyticus* cells in controlled microfluidic gradients and found that the strength of bacterial accumulation at the peak of a gradient was swimming-speed dependent.

An additional mode of flagella-mediated movement has been described in bacteria using a single polar flagellum whereby cells wrap their flagellum around their body and swim in a screw-like motion to navigate through microenvironments (Kühn et al., 2017). Although this form of motility is unlikely to occur in the water column it could be advantageous in marine sediments (Kühn et al., 2017) and has also been identified in marine symbionts (Kinosita et al., 2018) suggesting that it might play a role in symbiosis by aiding in host colonization (Raina et al., 2019). This alternative screw-like motion also indicates that there might be many other models of bacterial motility that are yet to be described.

Motile archaea explore marine seascapes by alternating forward and reverse swimming motions as the archaellum switches from clockwise to counter-clockwise rotation (Alam and Oesterhelt, 1984; Kinosita et al., 2016; Shahapure et al., 2014). In the absence of stimuli, the best-studied motile archaea *Halobacterium salinarum* and *Haloferax volcanii* perform a random walk (Hildebrand and Schimz, 1986; Quax et al., 2018) with swimming patterns more similar to the run-reverse-and-flick motion of *V. alginolyticus* (Xie et al., 2011) than to the run-and-tumble swimming of *E. coli*.

The higher chemotactic efficiency of marine bacteria might also result from differential signal transduction but this possibility has been not been thoroughly explored yet. The signal processing of marine bacteria has been suggested to be much faster than that of *E. coli* in order to allow the detection of chemical gradients at higher swimming speeds and this might translate into a higher turning frequency (Barbara and Mitchell, 2003; Mitchell et al., 1996; Seymour et al., 2009a). In addition, it has been revealed that marine bacteria operate close to the theoretical limits of chemotactic precision allowing them to aggregate in microscale regions of high DOM concentration before these diffuse to background levels (Brumley et al., 2019).

The ocean imposes unique environmental constraints on chemotaxis including low nutrient concentrations, ephemeral gradients, and pervasive flow. It is thus not surprising that marine bacteria exhibit strong phenotypic differences compared to enteric bacteria such as *E. coli* in the form of higher swimming speeds, different shapes, unique motility patterns, and higher levels of chemotactic performance.

# 5. Recent insight from omics data

During the past 15 years, marine microbiology has been transformed by the advent of genomic approaches, which have provided unprecedented insights into the taxonomic and functional diversity of marine microbial communities (DeLong and Karl, 2005; Sunagawa et al., 2015). Notably, these studies have also confirmed that genes involved in motility and chemotaxis are common, and their abundance is dynamic in marine bacterial communities.

## 5.1 Genomes of marine bacteria

While the most abundant clade of marine bacteria, *Pelagibacter ubique* (Giovannoni, 2017; Morris et al., 2002), is non-motile (Giovannoni et al., 2005) the genomes of many other marine bacteria, isolated from a wide variety of marine environments, frequently harbor genes involved in chemotaxis and motility (Gifford et al., 2013; Glöckner et al., 2003; López-Pérez et al., 2012; Ruby et al., 2005; Sunagawa et al., 2015; Thomas et al., 2008; Weiner et al., 2008). In particular, chemotaxis genes occur in multiple copies in many marine bacteria (Hamer et al., 2010) but are also found in archaea although less frequently (Salah Ud-Din and Roujeinikova, 2017). According to a survey of sequenced genomes, aquatic bacteria typically

contain a higher degree of duplication of genes associated with chemotaxis than bacteria that inhabit more environmentally stable environments (Alexandre et al., 2004).

Not surprisingly, chemotaxis genes are also abundant in the genomes of marine bacteria associated with animal hosts and organic surfaces attesting to the importance of active, directed motility in reaching these microenvironments (Raina et al., 2019; Gosink et al., 2002; Ruby et al., 2005; Thomas et al., 2008). These genes play a role in the colonization processes of both symbionts and pathogens. Chemotaxis and motility abilities are essential for the attachment of the bacterial symbiont *Marinobacter adhaerens* to its diatom host *Thalassiosira weissflogii* (Sonnenschein et al., 2012). In the bacterial fish pathogen *Edwardsiella tarda*, deletion of flagellar genes decreased its pathogenicity to zebrafish directly linking motility with the capacity of this pathogen to infect its host (Xu et al., 2014).

In some cases, the apparent absence of identifiable swimming and chemotaxis genes in the genomes of marine bacteria is equally illuminating. For instance, the model bacterium *Ruegeria pomeroyi* DSS-3 belongs to the *Roseobacter* clade, a group that commonly occurs in association with phytoplankton cells (Landa et al., 2017; Riemann et al., 2000) and often exhibits strong chemotactic performances (Miller and Belas, 2006; Miller et al., 2004; Seymour et al., 2009b, 2010a). Analysis of *R. pomeroyi*'s genome has revealed the presence of genes involved in motility as well as in a suite of functions that are typically used for the organism's association with plankton and particles (Moran et al., 2004). While these characteristics all point to an organism that is likely to use chemotaxis to exploit microscale gradients, *R. pomeroyi*'s genome contains no homologs of known proteins involved in chemotaxis (Moran et al., 2004). Similarly, analysis of the genome of the marine non-flagellated motile cyanobacterium *Synechococcus* WH8102, which is chemotactic towards nitrogenous compounds (Willey and Waterbury, 1989) has revealed that two unique large cell surface proteins are required for its motility: SwmA and SwmB (McCarren and Brahamsha, 2007; McCarren et al., 2005). These findings suggest that marine bacteria may harbor as yet unrecognized motility and chemotaxis systems.

## 5.2 Metagenomics

Metagenomic surveys of marine microbial assemblages have revealed that the occurrence of chemotaxis and motility genes is strongly affected by environmental conditions (Dinsdale et al., 2008; Vega Thurber et al., 2009). Depth-related shifts in the occurrence of motility and chemotaxis genes were observed in a metagenomic analysis of the water column in the North Pacific Ocean with higher representation of these genes in the photic zone (DeLong et al., 2006). This is consistent with the greater abundance of

microenvironments enriched with phytoplankton-produced organic matter within the upper, sunlit layers of the ocean. However, the more recent and much larger *Tara Oceans* campaign, which analyzed metagenomics data from 68 sites in epipelagic and mesopelagic waters across the globe revealed a significant enrichment of chemotaxis and motility genes directly below the photic zone (twilight zone) (Sunagawa et al., 2015). This enrichment of chemotaxis and motility genes is potentially of great utility to bacteria in the deep ocean to find and attach to sinking marine particles and aggregates but also to decrease their chance of encountering grazing predators (Matz and Jürgens, 2005). The latter argument stands in contrast with the general understanding that swimming tends to increase encounters including with predators (Kiørboe, 2008) highlighting instead the mechanism by which motility may help a bacterium escape from a predator upon capture.

Metagenomics has also provided access to the genomes of uncultured microbes (Rusch et al., 2007; Venter et al., 2004). For example, members of the globally abundant Marine Group II archaea (order *Candidatus* Poseidoniales) harbor genes involved in motility, adhesion, and oligosaccharide degradation (Rinke et al., 2019; Tully, 2019). These genomic capabilities suggest that members of the MGII archaea have a motile heterotrophic lifestyle exploiting oligosaccharide hotspots (e.g., phycospheres, particles) in the photic zone.

Metagenomics has shown that environmental variability can lead to shifts in the occurrence of motility and chemotaxis. Large increases in the abundance of motility and chemotaxis genes have been reported in coral-associated bacteria following temperature increases (Vega Thurber et al., 2009). These observations suggest that the prevalence of motility and chemotaxis varies strongly according to the physical and chemical features of specific marine habitats. Similarly, chemotaxis and motility gene abundance and regulation in the coral-associated microbiome is highly dependent on fine-scale chemical gradients emanating from the surfaces of corals ultimately impacting the microbial community structure of corals (Tout et al., 2014).

Perhaps one of the most intriguing observations relating to chemotaxis arising from metagenomic studies comes from a comparison of microbial and viral metagenomes across different environments (Dinsdale et al., 2008). High levels of proteins associated with motility and chemotaxis were observed in several viral metagenomes, which the authors suggest were not randomly acquired by the viral community. The role, if any, of these proteins in the phage is not clear but these observations indicate the potential for the horizontal transfer of genes involved in chemotaxis between different marine bacteria through phage infection.

## 5.3 Metatranscriptomics

Marine metatranscriptomic studies have shown that changing physicochemical conditions can shift the relative expression of motility and chemotaxis genes and have provided new insights into the processes determining when and where bacterial chemotaxis is most prevalent in the ocean. A temporal metatranscriptomic study of a coastal microbial assemblage revealed that transcripts for motility and chemotaxis followed both seasonal and daily patterns with higher levels of expression during the night (Gilbert et al., 2010). Daily variations in transcription of genes for motility and chemotaxis may be associated with shifts in phytoplankton exudation rates or particulate organic carbon (POC) production, which would be consistent with previous direct measurements showing that increased bacterial motility levels in the early evening are correlated with POC production (Grossart et al., 2001). In a similar manner, significant up-regulation of transcripts related to motility and chemotaxis have been recorded after addition of dissolved organic substrates to a marine bacterial assemblage (McCarren et al., 2010) and after enrichment of a water sample from the North Pacific Subtropical Gyre with nutrient-rich deep-sea water (Shi et al., 2012).

Observations of increased expression of motility and chemotaxis genes in nutrient-amended samples are consistent with previous direct observations of increased bacterial motility following enrichment (Mitchell et al., 1995a, 1995b). In both metatranscriptomic studies (McCarren et al., 2010; Shi et al., 2012) the increase in expression of motility and chemotaxis genes upon amendment occurred in parallel with an overall shift in community composition with a substantial increase in an *Alteromonas*-like population. This provides support for the hypothesis that increases in motility following enrichment are driven by shifts in community composition rather than directly by upregulation of expression in individuals. In contrast, expression of motility transcripts is decreased following bulk addition of DMSP (Vila-Costa et al., 2010). This finding is in line with observations that bulk additions of DMSP decrease bacterial chemotaxis to DMSP (Miller et al., 2004). These responses potentially occur because bulk DMSP additions eclipse the microscale DMSP cues surrounding individual phytoplankton cells decreasing the viability of chemotaxis as a strategy to find and exploit DMSP-rich hotspots (Seymour et al., 2010a).

Temperature is another environmental variable that can influence expression of chemotaxis and motility genes. For example, the marine bacterium *Photobacterium damselae* subsp. *damselae*, a facultative pathogen causing disease in fish and marine mammals, upregulates the expression of chemotaxis and

flagellar genes at higher temperature (Matanza and Osorio, 2018). This is correlated with higher expression of virulence genes (Matanza and Osorio, 2018), which highlights the importance of motility and chemotaxis in bacterial pathogenicity. In addition, increasing water temperatures considerably augment the performance of the coral pathogen *Vibrio coralliilyticus* in tracking the chemical signals of its coral host, *Pocillopora damicornis* (Garren et al., 2016). Indeed, when water temperature exceeded 30℃ the pathogen increased its chemotactic performance by >60%, and its swimming speed by >57% (Garren et al., 2016) substantially enhancing its ability to find its host.

The dynamic patterns in the occurrence of motility and chemotaxis genes in ocean metagenomes and transcriptomes confirm that these phenotypes are ecologically important features of natural marine bacterial assemblages that are often tightly coupled to the physicochemical nature of the environment.

# 6. Influence of microscale gradients on large-scale processes

The physical, chemical, and biological processes that we have described above all take place over small spatial scales (micrometer) and short time periods (seconds to minutes). However, they underpin the behavior, physiology, ecological relationships, and genomic characteristics of planktonic marine microorganisms. An important question to answer is, do processes occurring at the microscale in the heterogeneous seascape inhabited by marine bacteria have large-scale impacts? Or can we instead neglect this heterogeneity and consider that its impact will "average out" over larger scales?

## 6.1 Impacts on oceanic primary production

The productivity of the marine food web is governed by phytoplankton primary production, which means that interactions that directly affect phytoplankton growth have fundamental importance for ocean-scale processes. In addition to being controlled by dissolved nutrient availability in the bulk seawater phytoplankton growth is also influenced by processes occurring in the microenvironment surrounding their cells (i.e. the phycosphere). Reciprocal interactions with specific bacterial partners played out within this microenvironment can profoundly influence the provision of limiting nutrients and other essential growth factors to phytoplankton cells. In its simplest form, this reciprocal exchange can involve the uptake of exuded photosynthates (e.g. sugars) by the bacteria and the return of inorganic nutrients back to the phytoplankton cell (Azam and Malfatti, 2007). However, more complex and specific chemical exchanges have been uncovered involving bacterial synthesis of important minerals, B-vitamins, and

growth promoting hormones (Amin et al., 2009, 2012; Croft et al., 2005) that affect the growth and survival of phytoplankton cells.

Some microscale interactions may also negatively affect primary production in the ocean. Bacteria may outcompete phytoplankton for nutrients (Currie and Kalff, 1984) while specific bacteria can inhibit phytoplankton cell division (van Tol et al., 2017) or produce algicidal compounds that kill these primary producers (Barak-Gavish et al., 2018; Furusawa et al., 2011; Seyedsayamdost et al., 2011). When considering the cumulative impact of these positive and negative relationships, it is clear that these microscale interactions between phytoplankton and bacteria influence phytoplankton growth and are a determinant of primary production in the ocean, ultimately affecting the functioning and productivity of marine ecosystems.

## 6.2 Impacts on symbiont recruitment

The acquisition of microbial symbionts enables host organisms to expand their metabolic capabilities, inhabit otherwise hostile environments, and carve new ecological niches, which promotes species diversity and ecosystem services (Margulis, 1981; Ochman and Moran, 2001). Many important marine symbioses such as those of corals, tube worms, squid, mussels, protists, and phytoplankton rely on the acquisition of microbial partners from the environment (Raina et al., 2019). The importance of bacterial motility and chemotaxis in the establishment and maintenance of symbiotic interactions is well established in a small number of model systems but is likely to be important across a wide range of hosts (Raina et al., 2019). One of the most well-studied model systems in the marine environment is the symbiosis between the bioluminescent bacterium *Aliivibrio fischeri* and the Hawaiian bobtail squid (*Euprymna scolopes*) where the host uses the light produced by the symbionts as camouflage against predators during its nocturnal foraging (Nyholm et al., 2000). In the few hours following hatching, bacterial symbionts are selectively taken up from the environment (Nyholm and McFall-Ngai, 2004) and actively migrate towards the pores of the light organ using chemotaxis (Mandel et al., 2012). Another example of the use of motility and chemotaxis to recruit symbiotic partners is the marine macroalga *Ulva mutabilis*, which attracts its growth-enhancing symbiont *Roseovarius* by releasing the chemoattractant DMSP (Kessler et al., 2018). In addition, chemotaxis- and motility-deficient mutants of *Marinobacter adhaerens* were unable to locate and attach to their phytoplankton partners, negatively impacting the growth of the algal cells (Sonnenschein et al., 2012) and implying that chemotaxis is key to the establishment of a symbiotic exchange between bacteria and phytoplankton cells. As evidence of the

ecological importance of symbioses to the fitness and survival of key marine organisms continues to emerge, the chemotactic encounter of symbiotic partners is likely to be a pervasive mechanism.

## 6.3 Impacts on rates of chemical transformations

The behavioral responses of marine microorganisms to microscale heterogeneity in the water column are predicted to strongly affect the rates of carbon cycling through the base of the marine food web. Results derived from both experimental observations and mathematical models suggest that chemotaxis and motility significantly increase bacterial uptake rates of dissolved organic carbon (DOC) (Blackburn et al., 1997, 1998; Fenchel, 2002; Smriga et al., 2016; Stocker et al., 2008). It is important to note that even in the absence of chemotactic bacteria, DOC derived from hotspots would ultimately diffuse into the bulk seawater and become available to non-chemotactic bacteria. This suggests that, while the rates of DOC uptake may increase due to chemotaxis, the absolute amounts of carbon cycled may not change (Stocker, 2012; Stocker and Seymour, 2012). However, behavioral exploitation of microscale DOC hotspots might enhance total carbon flux if these elevated concentrations of organic compounds support an increase in bacterial growth efficiency (Azam and Malfatti, 2007). This process would ultimately lead to a higher proportion of DOC being converted into biomass and would therefore channel more carbon into the marine food web.

## 6.4 Impacts on exchanges between ocean and atmosphere

A large variety of biogenic volatile organic compounds (BVOCs) are produced by marine microorganisms and emitted to the atmosphere (Lawson et al., 2020; Moore et al., 2020). One of the best studied volatile compounds is the sulfur-containing dimethyl sulfide (DMS) because its release into the atmosphere represents the largest flux of biogenic sulfur on Earth and its subsequent oxidation forms sulfate aerosols that act as cloud condensation nuclei (Sievert et al., 2007; Simó, 2001). The precursor of this gas is DMSP, which is produced in high concentrations by many phytoplankton taxa (with intracellular concentration reaching 1–2 M) (Caruana and Malin, 2014; Keller, 1989). At the scale of bacteria, large concentrations of DMSP are introduced into the environment via point source events including exudation into the phycosphere, viral lysis, and grazing events (Seymour et al., 2010a). Given the diffusivity of this molecule and its high concentration in patches, it is perhaps not surprising that DMSP is a potent chemoattractant for many species of marine bacteria (Garren et al., 2014; Miller et al., 2004; Seymour et al., 2010a; Zimmer-Faust et al., 1996). In addition, DMSP is also an important growth substrate, supporting up to 13% of the bacterial carbon demand and nearly all their reduced sulfur needs

in surface waters (Kiene et al., 2000). However, not all marine bacteria use DMSP in the same way: some demethylate this compound to assimilate its sulfur and carbon into their cell (Howard et al., 2006) whereas others cleave DMSP and thereby produce the volatile DMS (Curson et al., 2011). These two competing pathways are often both present in marine bacteria (Curson et al., 2011) and chemotaxis toward DMSP has been demonstrated among bacterial strains that employ both the cleavage and demethylation pathways (Miller et al., 2004; Seymour et al., 2010a).

Twenty years ago, the DMSP availability hypothesis proposed that the relative importance of the two DMSP degradation pathways – and thus the amount of DMS produced – is regulated by the DMSP concentration in the environment (Kiene et al., 2000). According to this hypothesis, the utilization of DMSP in concentrated patches leads to the production of more DMS compared to utilization in dilute background concentrations. This long-standing hypothesis was recently validated experimentally confirming that external DMSP concentration dictates the relative expression of the two pathways with an increase in DMSP cleavage (and therefore DMS production) measured close to the surface of phytoplankton (Gao et al., 2020). Bacterial exploitation of microscale DMSP hotspots such as the phycosphere surrounding a DMSP-producing phytoplankton cell, which is governed by motility and chemotaxis, is thus likely to be an important determinant of the release of sulfur into the atmosphere as DMS, influencing the cycling of sulfur.

## 6.5 Impacts on exchanges between ocean and sediments

The flux of sinking particles from the sunlit upper ocean to the deep ocean forms the basis of the biological carbon pump, which leads to the sequestration of carbon into marine sediments for millennia (Ducklow et al., 2001). This vertical carbon flux is responsible for the export of more than 50 Gt of carbon per year. From the perspective of a planktonic bacterium, sinking organic particles represent a localized resource hotspot. As particles sink they are colonized and degraded by marine bacteria, which recycle the carbon they contain. Due to bacterial degradation only 25% of the organic particles sink deeper than the photic zone and only 1% reach the ocean floor (Azam and Long, 2001; Cho and Azam, 1988). These particles are thus hotspots of microbial activity that influence the global biogeochemical cycles of carbon and nitrogen.

The decomposition of sinking particles involves specific behavioral and metabolic responses by marine bacteria and archaea. As discussed above (section 2), motility and chemotaxis enhance the rate of encounter with particles by a factor of 100 to 1000 (Kiørboe and Jackson, 2001; Kiørboe et al., 2001;

Lambert et al., 2019). Observations of community assembly on model particles revealed a strong correlation between trophic level and motility (Datta et al., 2016). Early colonizers (arriving less than 48 hours after the exposure of particles to seawater) were not only motile and chemotactic but were also primary degraders of polymers (Datta et al., 2016). Conversely, late colonizers relied on metabolites from primary degraders to sustain their growth and were non-motile (Datta et al., 2016). These microscale processes have large-scale implications for carbon cycling because they directly control the quantity of particulate carbon that reach the seafloor (Buesseler et al., 2007).

The metabolic activity of microbes on particles creates strong and persistent micrometer- to millimeter-scale oxygen gradients (Paerl and Prufert, 1987). Important nitrogen transformation processes generally occur near oxic interfaces. As a result, particles are likely to support microscale partitioning of bacteria involved in nitrification (aerobic), denitrification (anaerobic), and nitrogen fixation (anaerobic) (Alldredge and Cohen, 1987; Glud et al., 2015; Paerl and Prufert, 1987). High levels of both nitrification and denitrification have been measured in organic aggregates derived from cyanobacteria (Klawonn et al., 2015). Similarly, direct stimulation of $N_2$ fixation has been measured in the presence of particles (Pedersen et al., 2018; Rahav et al., 2016) indicating that particles also represent important microscale hotspots for nitrogen cycling in the water column.

In summary, microbial processes occurring at the microscale in response to chemical gradients directly influence phytoplankton primary productivity, the recruitment of symbionts, the rate of biogeochemical transformations, the production of climate-active molecules, the cycling of limiting elements, and the long-term storage of carbon in the ocean. When reconsidering the question, does microscale heterogeneity matter, we can therefore safely answer in the affirmative. Microscale processes must be considered if we wish to achieve an accurate mechanistic understanding and realistic models of large-scale oceanic processes (Azam, 1998; Stocker, 2012).

## 7. Summary and future directions

- From the viewpoint of bacteria, seawater contains many nutrient hotspots and microhabitats that are either ephemeral or persistent. These hotspots arising from different micro- and macroorganisms, sinking particles, and decaying organic matter represent resource islands that can be exploited by copiotrophic bacteria for their growth.

- The physics of fluid dynamics and its impact on microorganisms at the microscale diverges from that ruling larger geophysical phenomena. In a world mostly dominated by diffusion the microscale remains relatively unaffected by turbulence allowing the steady emission of chemical gradients that are accessible for uptake by heterotrophic microorganisms. Turbulence enhances microscale heterogeneity by stirring nutrients in the water column and creating microscopic nutrient filaments.

- The large distances separating microorganisms in the water column, relative to their body size, renders nutrient uptake highly challenging if it only relies on random encounters. Heterotrophic bacteria have therefore evolved active behaviors such as high-speed motility and sensitive chemotaxis to increase the frequency at which they encounter resource hotspots. The performance of marine bacteria differs from that of the well-studied enteric model organisms and has been demonstrated to yield higher profitability, through higher swimming speeds, efficient swimming patterns, and directed chemotaxis.

- The ocean's microscale seascape gives rise to a diverse range of interactions within multiple microhabitats such as the phycosphere or sinking marine particles. Gradients also mediate interactions between microorganisms and larger eukaryotes, such as corals and fishes, directly impacting the ecology and dynamics of the oceans.

- Although microscale behaviors and interactions may happen within a fraction of a drop of seawater, they have global-scale consequences. The impacts of these interactions do not average out over larger scales but instead microbial cycling of chemicals often occurs exclusively within localized microenvironments.

As we become more aware of the microscale complexity of bacterial behaviors and interactions ruling the foundations of marine microbial ecology and their global impact on biogeochemical cycles, it appears that the scale of classic sampling techniques used in oceanography (e.g., Niskin bottles) is fundamentally disconnected from the microscale interactions at work. New technologies and mathematical models (Słomka et al., 2020; Słomka and Stocker, 2020) have been developed to decipher the microbial ecology of our oceans at more realistic scales. Single-cell genomics is beginning to reveal heterogeneity in gene expression (Blainey, 2013; Gao et al., 2020; Kalisky and Quake, 2011). Raman microscopy and mass-spectrometry imaging now allow measurement of the chemical signatures of individual cells (Lee et al., 2019, 2020). Atomic-force and electron microscopy are revealing the structural characteristics and the

spatial configuration of cells (Mittelviefhaus et al., 2019; Turner et al., 2016). In addition, developments in microfluidics now allow researchers to unravel microbial behavior in response to chemical landscapes in the laboratory (Behrendt et al., 2020; Salek et al., 2019; Seymour et al., 2010a, 2010b; Stocker et al., 2008) and directly *in situ* (Clerc et al., 2020; Lambert et al., 2017; Tout et al., 2015).

Despite these advances, key parameters needed to understand the survival of microbes in a sea of gradients are still poorly characterized. Work is required to determine (i) the fraction of motile bacteria in the ocean and how this fluctuates with daily cycles, seasons, nutrient abundance, and ocean depth; (ii) the principal chemical currencies in the water column used for growth or as signaling molecules and their impact on microbial community assembly and composition; (iii) the distribution of particle sizes and abundance through the water column and their impact on rates of bacterial encounter, degradation, and remineralization; and (iv) the variables that drive relations between heterogeneity and diversity, motility, and chemotaxis. Obtaining realistic estimates of these parameters that truly represent the heterogeneity of the oceans will not be easy, but the payoff will be a better understanding of the exquisite adaptations of bacteria and archaea to the complexity of marine environments and their contributions to the element cycles and climate of our planet.

## 8. References


Aaronson, S. (1978). Excretion of organic matter by phytoplankton in vitro. Limnol. Oceanogr. *23*, 838–838.

Ahmed, T., and Stocker, R. (2008). Experimental verification of the behavioral foundation of bacterial transport parameters using microfluidics. Biophys. J. *95*, 4481–4493.

Alam, M., and Oesterhelt, D. (1984). Morphology, function and isolation of halobacterial flagella. J. Mol. Biol. *176*, 459–475.

Alam, M., Claviez, M., Oesterhelt, D., and Kessel, M. (1984). Flagella and motility behaviour of square bacteria. EMBO J. *3*, 2899–2903.

Albers, S.-V., and Jarrell, K.F. (2018). The archaellum: an update on the unique archaeal motility structure. Trends Microbiol. *26*, 351–362.

Alexandre, G., Greer-Phillips, S., and Zhulin, I.B. (2004). Ecological role of energy taxis in microorganisms. FEMS Microbiol. Rev. *28*, 113–126.

Alldredge, A.L., and Cohen, Y. (1987). Can microscale chemical patches persist in the sea? Microelectrode Study of Marine Snow, Fecal Pellets. Science *235*, 689–691.

1427 Alldredge, A.L., and Gotschalk, C.C. (1990). The relative contribution of marine snow of different origins
1428 to biological processes in coastal waters. Cont. Shelf Res. *10*, 41–58.

1429 Alldredge, A.L., and Silver, M.W. (1988). Characteristics, dynamics and significance of marine snow.
1430 Prog. Oceanogr. *20*, 41–82.

1431 Alldredge, A.L., Passow, U., and Logan, B.E. (1993). The abundance and significance of a class of large,
1432 transparent organic particles in the ocean. Deep Sea Res. Part Oceanogr. Res. Pap. *40*, 1131–1140.

1433 Aluwihare, L.I., Repeta, D.J., and Chen, R.F. (1997). A major biopolymeric component to dissolved
1434 organic carbon in surface sea water. Nature *387*, 166–169.

1435 Amin, S.A., Green, D.H., Hart, M.C., Küpper, F.C., Sunda, W.G., and Carrano, C.J. (2009). Photolysis of
1436 iron–siderophore chelates promotes bacterial–algal mutualism. Proc. Natl. Acad. Sci. *106*, 17071–17076.

1437 Amin, S.A., Parker, M.S., and Armbrust, E.V. (2012). Interactions between diatoms and bacteria.
1438 Microbiol. Mol. Biol. Rev. MMBR *76*, 667–684.

1439 Amon, R.M.W., Fitznar, H.-P., and Benner, R. (2001). Linkages among the bioreactivity, chemical
1440 composition, and diagenetic state of marine dissolved organic matter. Limnol. Oceanogr. *46*, 287–297.

1441 Anand, G.S., Goudreau, P.N., and Stock, A.M. (1998). Activation of methylesterase CheB: evidence of a
1442 dual role for the regulatory domain. Biochemistry *37*, 14038–14047.

1443 Ankrah, N.Y.D., May, A.L., Middleton, J.L., Jones, D.R., Hadden, M.K., Gooding, J.R., LeCleir, G.R.,
1444 Wilhelm, S.W., Campagna, S.R., and Buchan, A. (2014). Phage infection of an environmentally relevant
1445 marine bacterium alters host metabolism and lysate composition. ISME J. *8*, 1089–1100.

1446 Arnosti, C. (2004). Speed bumps and barricades in the carbon cycle: substrate structural effects on carbon
1447 cycling. Mar. Chem. *92*, 263–273.

1448 Azam, F. (1998). Microbial control of oceanic carbon flux: the plot thickens. Science *280*, 694–696.

1449 Azam, F., and Ammerman, J.W. (1984). Cycling of organic matter by bacterioplankton in pelagic marine
1450 ecosystems: microenvironmental considerations. In Flows of Energy and Materials in Marine
1451 Ecosystems: Theory and Practice, M.J.R. Fasham, ed. (Boston, MA: Springer US), pp. 345–360.

1452 Azam, F., and Long, R.A. (2001). Sea snow microcosms. Nature *414*, 495–498.

1453 Azam, F., and Malfatti, F. (2007). Microbial structuring of marine ecosystems. Nat. Rev. Microbiol. *5*,
1454 782–791.

1455 Banerjee, A., Tsai, C.-L., Chaudhury, P., Tripp, P., Arvai, A.S., Ishida, J.P., Tainer, J.A., and Albers, S.-
1456 V. (2015). FlaF Is a β-sandwich protein that anchors the archaellum in the archaeal cell envelope by
1457 binding the S-layer protein. Structure *23*, 863–872.

1458 Barak-Gavish, N., Frada, M.J., Ku, C., Lee, P.A., DiTullio, G.R., Malitsky, S., Aharoni, A., Green, S.J.,
1459 Rotkopf, R., Kartvelishvily, E., et al. (2018). Bacterial virulence against an oceanic bloom-forming
1460 phytoplankter is mediated by algal DMSP. Sci. Adv. *4*, eaau5716.

1461 Barbara, G.M., and Mitchell, J.G. (2003). Bacterial tracking of motile algae. FEMS Microbiol. Ecol. *44*,
1462 79–87.

Bar-On, Y.M., Phillips, R., and Milo, R. (2018). The biomass distribution on Earth. Proc. Natl. Acad. Sci. *115*, 6506–6511.

Bassler, B.L., Gibbons, P.J., Yu, C., and Roseman, S. (1991). Chitin utilization by marine bacteria. Chemotaxis to chitin oligosaccharides by *Vibrio furnissii*. J. Biol. Chem. *266*, 24268–24275.

Behrendt, L., Salek, M.M., Trampe, E.L., Fernandez, V.I., Lee, K.S., Kühl, M., and Stocker, R. (2020). PhenoChip: A single-cell phenomic platform for high-throughput photophysiological analyses of microalgae. Sci. Adv. *6*, eabb2754.

Bell, W., and Mitchell, R. (1972). Chemotactic and growth response of marine bacteria to algal extracellular products. Biol. Bull. *143*, 265–277.

Bell, W.H., Lang, J.M., and Mitchell, R. (1974). Selective stimulation of marine bacteria by algal extracellular products. Limnol. Oceanogr. *19*, 833–839.

Berg, H.C. (1993). Random walks in biology (Princeton University Press).

Berg, H.C. (2000). Motile behavior of bacteria. Phys. Today *53*, 24–29.

Berg, H.C. (2008). *E. coli* in motion (Springer, New York. doi:10.1007/b97370

Berg, H.C., and Brown, D.A. (1972). Chemotaxis in *Escherichia coli* analysed by three-dimensional tracking. Nature *239*, 500–504.

Berg, H.C., and Tedesco, P.M. (1975). Transient response to chemotactic stimuli in *Escherichia coli*. Proc. Natl. Acad. Sci. *72*, 3235–3239.

Biersmith, A., and Benner, R. (1998). Carbohydrates in phytoplankton and freshly produced dissolved organic matter. Mar. Chem. *63*, 131–144.

Birtel, J., and Matthews, B. (2016). Grazers structure the bacterial and algal diversity of aquatic metacommunities. Ecology *97*, 3472–3484.

Blackall, L.L., Wilson, B., and van Oppen, M.J.H. (2015). Coral-the world's most diverse symbiotic ecosystem. Mol. Ecol. *24*, 5330–5347.

Blackburn, N., Azam, F., and Hagström, Å. (1997). Spatially explicit simulations of a microbial food web. Limnol. Oceanogr. *42*, 613–622.

Blackburn, N., Fenchel, T., and Mitchell, J. (1998). Microscale nutrient patches in planktonic habitats shown by chemotactic bacteria. Science *282*, 2254–2256.

Blainey, P.C. (2013). The future is now: single-cell genomics of bacteria and archaea. FEMS Microbiol. Rev. *37*, 407–427.

Bonnain, C., Breitbart, M., and Buck, K.N. (2016). The ferrojan horse hypothesis: iron-virus interactions in the ocean. Front. Mar. Sci. *3*, 82.

Broadbent, A.D., and Jones, G.B. (2004). DMS and DMSP in mucus ropes, coral mucus, surface films and sediment pore waters from coral reefs in the Great Barrier Reef. Mar. Freshw. Res. *55*, 849–855.

Brumley, D.R., Carrara, F., Hein, A.M., Yawata, Y., Levin, S.A., and Stocker, R. (2019). Bacteria push the limits of chemotactic precision to navigate dynamic chemical gradients. Proc. Natl. Acad. Sci. *116*, 10792–10797.

Buchan, A., LeCleir, G.R., Gulvik, C.A., and González, J.M. (2014). Master recyclers: features and functions of bacteria associated with phytoplankton blooms. Nat. Rev. Microbiol. *12*, 686–698.

Buesseler, K.O., Lamborg, C.H., Boyd, P.W., Lam, P.J., Trull, T.W., Bidigare, R.R., Bishop, J.K.B., Casciotti, K.L., Dehairs, F., Elskens, M., et al. (2007). Revisiting carbon flux through the ocean's twilight zone. Science *316*, 567–570.

Burdige, D.J., and Gardner, K.G. (1998). Molecular weight distribution of dissolved organic carbon in marine sediment pore waters. Mar. Chem. *62*, 45–64.

Burdige, D.J., and Komada, T. (2015). Chapter 12 - Sediment pore waters. In Biogeochemistry of Marine Dissolved Organic Matter (Second Edition), D.A. Hansell, and C.A. Carlson, eds. (Boston: Academic Press), pp. 535–577.

Cai, R., Zhou, W., He, C., Tang, K., Guo, W., Shi, Q., Gonsior, M., and Jiao, N. (2019). Microbial processing of sediment-derived dissolved organic matter: implications for its subsequent biogeochemical cycling in overlying seawater. J. Geophys. Res. Biogeosciences *124*, 3479–3490.

Carini, P., Steindler, L., Beszteri, S., and Giovannoni, S.J. (2013). Nutrient requirements for growth of the extreme oligotroph '*Candidatus Pelagibacter ubique*' HTCC1062 on a defined medium. ISME J. *7*, 592–602.

Caruana, A.M.N., and Malin, G. (2014). The variability in DMSP content and DMSP lyase activity in marine dinoflagellates. Prog. Oceanogr. *120*, 410–424.

Chaban, B., Ng, S.Y.M., Kanbe, M., Saltzman, I., Nimmo, G., Aizawa, S.-I., and Jarrell, K.F. (2007). Systematic deletion analyses of the fla genes in the flagella operon identify several genes essential for proper assembly and function of flagella in the archaeon, *Methanococcus maripaludis*. Mol. Microbiol. *66*, 596–609.

Cho, B.C., and Azam, F. (1988). Major role of bacteria in biogeochemical fluxes in the ocean's interior. Nature *332*, 441–443.

Cirri, E., and Pohnert, G. (2019). Algae−bacteria interactions that balance the planktonic microbiome. New Phytol. *223*, 100–106.

Clerc, E.E., Raina, J.-B., Lambert, B.S., Seymour, J., and Stocker, R. (2020). In situ chemotaxis assay to examine microbial behavior in aquatic ecosystems. JoVE J. Vis. Exp. e61062.

Cole, J.J. (1982). Interactions between bacteria and algae in aquatic acosystems. Annu. Rev. Ecol. Syst. *13*, 291–314.

Conrad, J.C., Gibiansky, M.L., Jin, F., Gordon, V.D., Motto, D.A., Mathewson, M.A., Stopka, W.G., Zelasko, D.C., Shrout, J.D., and Wong, G.C.L. (2011). Flagella and pili-mediated near-surface single-cell motility mechanisms in *P. aeruginosa*. Biophys. J. *100*, 1608–1616.

1533 Copping, A.E., and Lorenzen, C.J. (1980). Carbon budget of a marine phytoplankton-herbivore system
1534 with carbon-14 as a tracer1. Limnol. Oceanogr. *25*, 873–882.

1535 Cremer, J., Honda, T., Tang, Y., Wong-Ng, J., Vergassola, M., and Hwa, T. (2019). Chemotaxis as a
1536 navigation strategy to boost range expansion. Nature *575* (7785), 658-663.

1537 Croft, M.T., Lawrence, A.D., Raux-Deery, E., Warren, M.J., and Smith, A.G. (2005). Algae acquire
1538 vitamin B12 through a symbiotic relationship with bacteria. Nature *438*, 90–93.

1539 Currie, D.J., and Kalff, J. (1984). A comparison of the abilities of freshwater algae and bacteria to acquire
1540 and retain phosphorus1. Limnol. Oceanogr. *29*, 298–310.

1541 Curson, A.R.J., Todd, J.D., Sullivan, M.J., and Johnston, A.W.B. (2011). Catabolism of
1542 dimethylsulphoniopropionate: microorganisms, enzymes and genes. Nat. Rev. Microbiol. *9*, 849–859.

1543 Datta, M.S., Sliwerska, E., Gore, J., Polz, M.F., and Cordero, O.X. (2016). Microbial interactions lead to
1544 rapid micro-scale successions on model marine particles. Nat. Commun. *7*, 11965.

1545 DeLong, E.F., and Karl, D.M. (2005). Genomic perspectives in microbial oceanography. Nature *437*,
1546 336–342.

1547 DeLong, E.F., Franks, D.G., and Alldredge, A.L. (1993). Phylogenetic diversity of aggregate-attached vs.
1548 free-living marine bacterial assemblages. Limnol. Oceanogr. *38*, 924–934.

1549 DeLong, E.F., Preston, C.M., Mincer, T., Rich, V., Hallam, S.J., Frigaard, N.-U., Martinez, A., Sullivan,
1550 M.B., Edwards, R., Brito, B.R., et al. (2006). Community genomics among stratified microbial
1551 assemblages in the ocean's interior. Science *311*, 496–503.

1552 Dinsdale, E.A., Edwards, R.A., Hall, D., Angly, F., Breitbart, M., Brulc, J.M., Furlan, M., Desnues, C.,
1553 Haynes, M., Li, L., et al. (2008). Functional metagenomic profiling of nine biomes. Nature *452*, 629–632.

1554 Doane, M.P., Morris, M.M., Papudeshi, B., Allen, L., Pande, D., Haggerty, J.M., Johri, S., Turnlund,
1555 A.C., Peterson, M., Kacev, D., et al. (2020). The skin microbiome of elasmobranchs follows
1556 phylosymbiosis, but in teleost fishes, the microbiomes converge. Microbiome *8*, 93.

1557 Ducklow, H., Steinberg, D., and Buesseler, K. (2001). Upper ocean carbon export and the biological
1558 pump. Oceanography *14*, 50–58.

1559 Dührkop, K., Shen, H., Meusel, M., Rousu, J., and Böcker, S. (2015). Searching molecular structure
1560 databases with tandem mass spectra using CSI:FingerID. Proc. Natl. Acad. Sci. U. S. A. *112*, 12580–
1561 12585.

1562 Durham, B.P., Sharma, S., Luo, H., Smith, C.B., Amin, S.A., Bender, S.J., Dearth, S.P., Van Mooy,
1563 B.A.S., Campagna, S.R., Kujawinski, E.B., et al. (2015). Cryptic carbon and sulfur cycling between
1564 surface ocean plankton. Proc. Natl. Acad. Sci. U. S. A. *112*, 453–457.

1565 Ebrahimi, A., Schwartzman, J., and Cordero, O.X. (2019). Cooperation and spatial self-organization
1566 determine rate and efficiency of particulate organic matter degradation in marine bacteria. Proc. Natl.
1567 Acad. Sci. *116*, 23309–23316.

Edwards, M.R., Carlsen, R.W., Zhuang, J., and Sitti, M. (2014). Swimming characterization of *Serratia marcescens* for bio-hybrid micro-robotics. J. Micro-Bio Robot. *9*, 47–60.

Elyakova, L.A., Pavlov, G.M., Isakov, V.V., Zaitseva, I.I., and Stepenchekova, T.A. (1994). Molecular characteristics of subfractions of laminarin. Chem. Nat. Compd. *30*, 273–274.

Emerson, S., and Hedges, J. (2008). Chemical oceanography and the marine carbon cycle (Cambridge University Press).

Engel, A., Thoms, S., Riebesell, U., Rochelle-Newall, E., and Zondervan, I. (2004). Polysaccharide aggregation as a potential sink of marine dissolved organic carbon. Nature *428*, 929–932.

Engel, A., Händel, N., Wohlers, J., Lunau, M., Grossart, H.-P., Sommer, U., and Riebesell, U. (2011). Effects of sea surface warming on the production and composition of dissolved organic matter during phytoplankton blooms: results from a mesocosm study. J. Plankton Res. *33*, 357–372.

Fenchel, T. (1994). Motility and chemosensory behaviour of the sulphur bacterium *Thiovulum majus*. Microbiology, *140*, 3109–3116.

Fenchel, T. (2001). Eppur si muove: many water column bacteria are motile. Aquat. Microb. Ecol. *24*, 197–201.

Fenchel, T. (2002). Microbial behavior in a heterogeneous world. Science *296*, 1068–1071.

Fenchel, T., and Thar, R. (2004). "*Candidatus Ovobacter propellens*": a large conspicuous prokaryote with an unusual motility behaviour. FEMS Microbiol. Ecol. *48*, 231–238.

Fenchel, T. and Finlay, B. (2008). Oxygen and the spatial structure of microbial communities. Biological Reviews, 83: 553-569.

Ferguson, R.L., and Sunda, W.G. (1984). Utilization of amino acids by planktonic marine bacteria: Importance of clean technique and low substrate additions1,2. Limnol. Oceanogr. *29*, 258–274.

Flynn, K.J., Clark, D.R., and Xue, Y. (2008). Modeling the release of dissolved organic matter by phytoplankton1. J. Phycol. *44*, 1171–1187.

Fogg, G.E. (1977). Excretion of organic matter by phytoplankton. Limnol. Oceanogr. *22*, 576–577.

Follett, C.L., Repeta, D.J., Rothman, D.H., Xu, L., and Santinelli, C. (2014). Hidden cycle of dissolved organic carbon in the deep ocean. Proc. Natl. Acad. Sci. *111*, 16706–16711.

Fontanez, K.M., Eppley, J.M., Samo, T.J., Karl, D.M., and DeLong, E.F. (2015). Microbial community structure and function on sinking particles in the North Pacific Subtropical Gyre. Front. Microbiol. *6*, 469.

Fossing, H., Gallardo, V.A., Jørgensen, B.B., Hüttel, M., Nielsen, L.P., Schulz, H., Canfield, D.E., Forster, S., Glud, R.N., Gundersen, J.K., et al. (1995). Concentration and transport of nitrate by the mat-forming sulphur bacterium *Thioploca*. Nature *374*, 713–715.

Furusawa, G., Yoshikawa, T., Yasuda, A., and Sakata, T. (2011). Algicidal activity and gliding motility of *Saprospira* sp. SS98-5. Can. J. Microbiol. *49*, 92-100.

Ganesh, S., Parris, D.J., DeLong, E.F., and Stewart, F.J. (2014). Metagenomic analysis of size-fractionated picoplankton in a marine oxygen minimum zone. ISME J. *8*, 187–211.

Gao, C., Fernandez, V.I., Lee, K.S., Fenizia, S., Pohnert, G., Seymour, J.R., Raina, J.-B., and Stocker, R. (2020). Single-cell bacterial transcription measurements reveal the importance of dimethylsulfoniopropionate (DMSP) hotspots in ocean sulfur cycling. Nat. Commun. *11*, 1942.

Gärdes, A., Iversen, M.H., Grossart, H.-P., Passow, U., and Ullrich, M.S. (2011). Diatom-associated bacteria are required for aggregation of *Thalassiosira weissflogii*. ISME J. *5*, 436–445.

Garren, M., Son, K., Raina, J.-B., Rusconi, R., Menolascina, F., Shapiro, O.H., Tout, J., Bourne, D.G., Seymour, J.R., and Stocker, R. (2014). A bacterial pathogen uses dimethylsulfoniopropionate as a cue to target heat-stressed corals. ISME J. *8*, 999–1007.

Garren, M., Son, K., Tout, J., Seymour, J.R., and Stocker, R. (2016). Temperature-induced behavioral switches in a bacterial coral pathogen. ISME J. *10*, 1363–1372.

Gifford, S.M., Sharma, S., Booth, M., and Moran, M.A. (2013). Expression patterns reveal niche diversification in a marine microbial assemblage. ISME J. *7*, 281–298.

Gilbert, J.A., Field, D., Swift, P., Thomas, S., Cummings, D., Temperton, B., Weynberg, K., Huse, S., Hughes, M., Joint, I., et al. (2010). The taxonomic and functional diversity of microbes at a temperate coastal site: A 'multi-omic' study of seasonal and diel temporal variation. PLOS ONE *5*, e15545.

Giovannoni, S.J. (2017). SAR11 Bacteria: The most abundant plankton in the oceans. Annu. Rev. Mar. Sci. *9*, 231–255.

Giovannoni, S.J., Tripp, H.J., Givan, S., Podar, M., Vergin, K.L., Baptista, D., Bibbs, L., Eads, J., Richardson, T.H., Noordewier, M., et al. (2005). Genome streamlining in a cosmopolitan oceanic bacterium. Science *309*, 1242–1245.

Glöckner, F.O., Kube, M., Bauer, M., Teeling, H., Lombardot, T., Ludwig, W., Gade, D., Beck, A., Borzym, K., Heitmann, K., et al. (2003). Complete genome sequence of the marine planctomycete *Pirellula* sp. strain 1. Proc. Natl. Acad. Sci. *100*, 8298–8303.

Glud, R.N., Grossart, H.-P., Larsen, M., Tang, K.W., Arendt, K.E., Rysgaard, S., Thamdrup, B., and Nielsen, T.G. (2015). Copepod carcasses as microbial hot spots for pelagic denitrification. Limnol. Oceanogr. *60*, 2026–2036.

Goldman, J.C., McCarthy, J.J., and Peavey, D.G. (1979). Growth rate influence on the chemical composition of phytoplankton in oceanic waters. Nature *279*, 210–215.

Gosink, K.K., Kobayashi, R., Kawagishi, I., and Häse, C.C. (2002). Analyses of the roles of the three CheA homologs in chemotaxis of *Vibrio cholerae*. J. Bacteriol. *184*, 1767–1771.

Granum, E. 2002. Metabolism and function of b-1,3-glucan in marine diatoms. PhD Thesis, Department of Biotechnology, Faculty of Natural Sciences and Technology, Norwegian University of Science and Technology (NTNU), Trondheim, Norway.

Granum, E., Kirkvold, S., and Myklestad, S.M. (2002). Cellular and extracellular production of carbohydrates and amino acids by the marine diatom Skeletonema costatum: diel variations and effects of N depletion. Mar. Ecol. Prog. Ser. *242*, 83–94.

Grossart, H.-P., and Simon, M. (1998). Bacterial colonization and microbial decomposition of limnetic organic aggregates (lake snow). Aquat. Microb. Ecol. *15*, 127–140.

Grossart, H., Riemann, L., and Azam, F. (2001). Bacterial motility in the sea and its ecological implications. Aquat. Microb. Ecol. *25*, 247–258.

Guadayol, Ò., Thornton, K.L. and Humphries, S., 2017. Cell morphology governs directional control in swimming bacteria. Scientific reports. *7*(1), 1-13.

Guasto, J.S., Rusconi, R., and Stocker, R. (2012). Fluid mechanics of planktonic microorganisms. Annu. Rev. Fluid Mech. *44*, 373–400.

Gude, S., Pinçe, E., Taute, K.M., Seinen, A.-B., Shimizu, T.S., and Tans, S.J. (2020). Bacterial coexistence driven by motility and spatial competition. Nature *578*, 588–592.

Guidi, L., Chaffron, S., Bittner, L., Eveillard, D., Larhlimi, A., Roux, S., Darzi, Y., Audic, S., Berline, L., and Brum, J.R. (2016). Plankton networks driving carbon export in the oligotrophic ocean. Nature *532*, 465–470.

Haas, A.F., and Wild, C. (2010). Composition analysis of organic matter released by cosmopolitan coral reef-associated green algae. Aquat. Biol. *10*, 131–138.

Hamer, R., Chen, P.-Y., Armitage, J.P., Reinert, G., and Deane, C.M. (2010). Deciphering chemotaxis pathways using cross species comparisons. BMC Syst. Biol. *4*, 3.

Hansell, D.A. (2013). Recalcitrant dissolved organic carbon fractions. Annu. Rev. Mar. Sci. *5*, 421–445.

Hansell, D.A., and Carlson, C.A. (1998). Net community production of dissolved organic carbon. Glob. Biogeochem. Cycles *12*, 443–453.

Hartmann, A.C., Petras, D., Quinn, R.A., Protsyuk, I., Archer, F.I., Ransome, E., Williams, G.J., Bailey, B.A., Vermeij, M.J.A., Alexandrov, T., et al. (2017). Meta-mass shift chemical profiling of metabolomes from coral reefs. Proc. Natl. Acad. Sci. *114*, 11685–11690.

Harwood, C.S., Fosnaugh, K., and Dispensa, M. (1989). Flagellation of *Pseudomonas putida* and analysis of its motile behavior. J. Bacteriol. *171*, 4063–4066.

Hellebust, J.A. (1965). Excretion of some organic compounds by marine phytoplankton. Limnol. Oceanogr. *10*, 192–206.

Herzog, B., and Wirth, R. (2012). Swimming behavior of selected species of archaea. Appl. Environ. Microbiol. *78*, 1670–1674.

Hess, J.F., Oosawa, K., Kaplan, N., and Simon, M.I. (1988). Phosphorylation of three proteins in the signaling pathway of bacterial chemotaxis. Cell *53*, 79–87.

Hildebrand, E., and Schimz, A. (1986). Integration of photosensory signals in *Halobacterium halobium*. J. Bacteriol. *167*, 305–311.

1673 Hirota, N., and Imae, Y. (1983). Na+-driven flagellar motors of an alkalophilic *Bacillus* strain YN-1. J.
1674 Biol. Chem. *258*, 10577–10581.

1675 Hodson, R.E., Azam, F., Carlucci, A.F., Fuhrman, J.A., Karl, D.M., and Holm-Hansen, O. (1981).
1676 Microbial uptake of dissolved organic matter in Mcmurdo Sound, Antarctica. Mar. Biol. *61*, 89–94.

1677 Hollibaugh, J.T., and Azam, F. (1983). Microbial degradation of dissolved proteins in seawater1. Limnol.
1678 Oceanogr. *28*, 1104–1116.

1679 Hook, A.L., Flewellen, J.L., Dubern, J.-F., Carabelli, A.M., Zaid, I.M., Berry, R.M., Wildman, R.D.,
1680 Russell, N., Williams, P., and Alexander, M.R. (2019). Simultaneous tracking of *Pseudomonas*
1681 *aeruginosa* motility in liquid and at the solid-liquid interface reveals differential roles for the flagellar
1682 stators. MSystems *4 (5)*.

1683 Howard, E.C., Henriksen, J.R., Buchan, A., Reisch, C.R., Bürgmann, H., Welsh, R., Ye, W., González,
1684 J.M., Mace, K., Joye, S.B., et al. (2006). Bacterial taxa that limit sulfur flux from the ocean. Science *314*,
1685 649–652.

1686 Hütz, A., Schubert, K., and Overmann, J. (2011). *Thalassospira* sp. isolated from the oligotrophic eastern
1687 Mediterranean Sea exhibits chemotaxis toward inorganic phosphate during starvation. Appl. Environ.
1688 Microbiol. *77*, 4412–4421.

1689 Isao, K., Hara, S., Terauchi, K., and Kogure, K. (1990). Role of sub-micrometre particles in the ocean.
1690 Nature *345*, 242–244.

1691 Jackson, G.A. (1980). Phytoplankton growth and zooplankton grazing in oligotrophic oceans. Nature *284*,
1692 439–441.

1693 Jackson, G.A. (1987). Simulating chemosensory responses of marine microorganisms. Limnol. Oceanogr.
1694 *32*, 1253–1266.

1695 Jackson, G.A. (1989). Simulation of bacterial attraction and adhesion to falling particles in an aquatic
1696 environment. Limnol. Oceanogr. *34*, 514–530.

1697 Jackson, G.A. (1990). A model of the formation of marine algal flocs by physical coagulation processes.
1698 Deep Sea Res. A *37*, 1197–1211.

1699 Jackson, G.A. (2012). Seascapes: the world of aquatic organisms as determined by their particulate
1700 natures. J. Exp. Biol. *215*, 1017–1030.

1701 Jacobsen, T.R., and Azam, F. (1984). Role of bacteria in copepod fecal pellet decomposition:
1702 colonization, growth rates and mineralization. Bull. Mar. Sci. *35*, 495–502.

1703 Jarrell, K.F., and Albers, S.-V. (2012). The archaellum: an old motility structure with a new name. Trends
1704 Microbiol. *20*, 307–312.

1705 Jarrell, K.F., Bayley, D.P., Florian, V., and Klein, A. (1996). Isolation and characterization of insertional
1706 mutations in flagellin genes in the archaeon *Methanococcus voltae*. Mol. Microbiol. *20*, 657–666.

1707 Jenkinson, I.R., Sun, X.X., and Seuront, L. (2015). Thalassorheology, organic matter and plankton:
1708 towards a more viscous approach in plankton ecology. J. Plankton Res. *37*, 1100–1109.

1709 Jiao, N., Herndl, G.J., Hansell, D.A., Benner, R., Kattner, G., Wilhelm, S.W., Kirchman, D.L.,
1710 Weinbauer, M.G., Luo, T., Chen, F., et al. (2010). Microbial production of recalcitrant dissolved organic
1711 matter: long-term carbon storage in the global ocean. Nat. Rev. Microbiol. *8*, 593–599.

1712 Johansen, J.E., Pinhassi, J., Blackburn, N., Zweifel, U.L., and Hagström, Å. (2002). Variability in motility
1713 characteristics among marine bacteria. Aquat. Microb. Ecol. *28*, 229–237.

1714 Johnson, A.R., Wiens, J.A., Milne, B.T., and Crist, T.O. (1992). Animal movements and population
1715 dynamics in heterogeneous landscapes. Landsc. Ecol. *7*, 63–75.

1716 Jones, A.K., and Cannon, R.C. (1986). The release of micro-algal photosynthate and associated bacterial
1717 uptake and heterotrophic growth. Br. Phycol. J. *21*, 341–358.

1718 Jørgensen, B.B., and Revsbech, N.P. (1983). Colorless sulfur bacteria, *Beggiatoa* spp. and *Thiovulum*
1719 spp., in $O_2$ and $H_2S$ microgradients. Appl. Environ. Microbiol. *45*, 1261–1270.

1720 Jørgensen, B.B., Findlay, A.J., and Pellerin, A. (2019). The biogeochemical sulfur cycle of marine
1721 sediments. Front. Microbiol. *10*, 849.

1722 Jover, L.F., Effler, T.C., Buchan, A., Wilhelm, S.W., and Weitz, J.S. (2014). The elemental composition
1723 of virus particles: implications for marine biogeochemical cycles. Nat. Rev. Microbiol. *12*, 519–528.

1724 Kaiser, K., and Benner, R. (2012). Organic matter transformations in the upper mesopelagic zone of the
1725 North Pacific: chemical composition and linkages to microbial community structure. J. Geophys. Res.
1726 Oceans *117* (C1).

1727 Kalisky, T., and Quake, S.R. (2011). Single-cell genomics. Nat. Methods *8*, 311–314.

1728 Kallmeyer, J., Pockalny, R., Adhikari, R.R., Smith, D.C., and D'Hondt, S. (2012). Global distribution of
1729 microbial abundance and biomass in subseafloor sediment. Proc. Natl. Acad. Sci. U. S. A. *109*, 16213–
1730 16216.

1731 Keller, M.D. (1989). Dimethyl sulfide production and marine phytoplankton: the importance of species
1732 composition and cell size. Biol. Oceanogr. *6*, 375–382.

1733 Kessler, R.W., Weiss, A., Kuegler, S., Hermes, C., and Wichard, T. (2018). Macroalgal–bacterial
1734 interactions: role of dimethylsulfoniopropionate in microbial gardening by *Ulva* (*Chlorophyta*). Mol.
1735 Ecol. *27*, 1808–1819.

1736 Khan, S., and Scholey, J.M. (2018). Assembly, functions and evolution of archaella, flagella and cilia.
1737 Curr. Biol. *28*, R278–R292.

1738 Kiene, R.P., Linn, L.J., and Bruton, J.A. (2000). New and important roles for DMSP in marine microbial
1739 communities. J. Sea Res. *43*, 209–224.

1740 Kim, C., Jackson, M., Lux, R., and Khan, S. (2001). Determinants of chemotactic signal amplification in
1741 *Escherichia coli*. Edited by I. B. Holland. J. Mol. Biol. *307*, 119–135.

1742 Kim, S., Kramer, R.W., and Hatcher, P.G. (2003). Graphical method for analysis of ultrahigh-resolution
1743 broadband mass spectra of natural organic matter, the van Krevelen diagram. Anal. Chem. *75*, 5336–
1744 5344.

1745 Kinosita, Y., Uchida, N., Nakane, D., and Nishizaka, T. (2016). Direct observation of rotation and steps
1746 of the archaellum in the swimming halophilic archaeon *Halobacterium salinarum*. Nat. Microbiol. *1*, 1–9.

1747 Kinosita, Y., Kikuchi, Y., Mikami, N., Nakane, D., and Nishizaka, T. (2018). Unforeseen swimming and
1748 gliding mode of an insect gut symbiont, *Burkholderia* sp. RPE64, with wrapping of the flagella around its
1749 cell body. ISME J. *12*, 838–848.

1750 Kiørboe, T. (2008). A mechanistic approach to plankton ecology (Princeton University Press).

1751 Kiørboe, T., and Jackson, G.A. (2001). Marine snow, organic solute plumes, and optimal chemosensory
1752 behavior of bacteria. Limnol. Oceanogr. *46*, 1309–1318.

1753 Kiørboe, T., Ploug, H., and Thygesen, U. (2001). Fluid motion and solute distribution around sinking
1754 aggregates. I. Small-scale fluxes and heterogeneity of nutrients in the pelagic environment. Mar. Ecol.
1755 Prog. Ser. *211*, 1–13.

1756 Kiørboe, T., Grossart, H.-P., Ploug, H., and Tang, K. (2002). Mechanisms and rates of bacterial
1757 colonization of sinking aggregates. Appl. Environ. Microbiol. *68*, 3996–4006.

1758 Klawonn, I., Bonaglia, S., Brüchert, V., and Ploug, H. (2015). Aerobic and anaerobic nitrogen
1759 transformation processes in $N_2$ -fixing cyanobacterial aggregates. ISME J. *9*, 1456–1466.

1760 Kühl, M., Cohen, Y., Dalsgaard, T., Jørgensen, B.B., and Revsbech, N.P. (1995). Microenvironment and
1761 photosynthesis of zooxanthellae in scleractinian corals studied with microsensors for $O_2$, pH and light.
1762 Mar. Ecol.-Prog. Ser. *117*, 159–172.

1763 Kühn, M.J., Schmidt, F.K., Eckhardt, B., and Thormann, K.M. (2017). Bacteria exploit a polymorphic
1764 instability of the flagellar filament to escape from traps. Proc. Natl. Acad. Sci. *114*, 6340–6345.

1765 Kujawinski, E.B., Longnecker, K., Barott, K.L., Weber, R.J.M., and Kido Soule, M.C. (2016). Microbial
1766 community structure affects marine dissolved organic matter composition. Front. Mar. Sci. *3*, 45.

1767 Lacal, J., García-Fontana, C., Muñoz-Martínez, F., Ramos, J.-L., and Krell, T. (2010). Sensing of
1768 environmental signals: classification of chemoreceptors according to the size of their ligand binding
1769 regions. Environ. Microbiol. *12*, 2873–2884.

1770 Lambert, B.S., Raina, J.-B., Fernandez, V.I., Rinke, C., Siboni, N., Rubino, F., Hugenholtz, P., Tyson,
1771 G.W., Seymour, J.R., and Stocker, R. (2017). A microfluidics-based in situ chemotaxis assay to study the
1772 behaviour of aquatic microbial communities. Nat. Microbiol. *2*, 1344–1349.

1773 Lambert, B.S., Fernandez, V.I., and Stocker, R. (2019). Motility drives bacterial encounter with particles
1774 responsible for carbon export throughout the ocean. Limnol. Oceanogr. Lett. *4*, 113–118.

1775 Lampert, W. (1978). Release of dissolved organic carbon by grazing zooplankton. Limnol. Oceanogr. *23*,
1776 831–834.

1777 Lancelot, C. (1984). Extracellular release of small and large molecules by phytoplankton in the Southern
1778 Bight of the North Sea. Estuar. Coast. Shelf Sci. *18*, 65–77.

1779 Landa, M., Burns, A.S., Roth, S.J., and Moran, M.A. (2017). Bacterial transcriptome remodeling during
1780 sequential co-culture with a marine dinoflagellate and diatom. ISME J. *11*, 2677–2690.

Lassak, K., Neiner, T., Ghosh, A., Klingl, A., Wirth, R., and Albers, S.-V. (2012). Molecular analysis of the crenarchaeal flagellum. Mol. Microbiol. *83*, 110–124.

Lauro, F.M., and Bartlett, D.H. (2008). Prokaryotic lifestyles in deep sea habitats. Extremophiles *12*, 15–25.

Lauro, F.M., McDougald, D., Thomas, T., Williams, T.J., Egan, S., Rice, S., DeMaere, M.Z., Ting, L., Ertan, H., Johnson, J., et al. (2009). The genomic basis of trophic strategy in marine bacteria. Proc. Natl. Acad. Sci. U. S. A. *106*, 15527–15533.

Lawson, C.A., Seymour, J.R., Possell, M., Suggett, D.J., and Raina, J.-B. (2020). The volatilomes of symbiodiniaceae-associated bacteria are influenced by chemicals derived from their algal partner. Front. Mar. Sci. *7*, 106.

Lee, K.S., Palatinszky, M., Pereira, F.C., Nguyen, J., Fernandez, V.I., Mueller, A.J., Menolascina, F., Daims, H., Berry, D., and Wagner, M. (2019). An automated Raman-based platform for the sorting of live cells by functional properties. Nat. Microbiol. *4*, 1035–1048.

Lee, K.S., Wagner, M., and Stocker, R. (2020). Raman-based sorting of microbial cells to link functions to their genes. Microb. Cell *7*, 62.

Lehman, J.T., and Scavia, D. (1982a). Microscale nutrient patches produced by zooplankton. Proc. Natl. Acad. Sci. U. S. A. *79*, 5001–5005.

Lehman, J.T., and Scavia, D. (1982b). Microscale Patchiness of Nutrients in Plankton Communities. Science *216*, 729–730.

Leifson, E., Cosenza, B.J., Murchelano, R., and Cleverdon, R.C. (1964). Motile marine bacteria. Techniques, ecology, and general characteristics. J. Bacteriol. *87*, 652–666.

Li, N., Kojima, S., and Homma, M. (2011). Sodium-driven motor of the polar flagellum in marine bacteria *Vibrio*. Genes Cells *16*, 985–999.

Lidbury, I., Murrell, J.C., and Chen, Y. (2014). Trimethylamine N-oxide metabolism by abundant marine heterotrophic bacteria. Proc. Natl. Acad. Sci. *111*, 2710–2715.

Liu, H., Nolla, H., and Campbell, L. (1997). Prochlorococcus growth rate and contribution to primary production in the equatorial and subtropical North Pacific Ocean. Aquat. Microb. Ecol. *12*, 39–47.

Liu, Q., Lu, X., Tolar, B.B., Mou, X., and Hollibaugh, J.T. (2015). Concentrations, turnover rates and fluxes of polyamines in coastal waters of the South Atlantic Bight. Biogeochemistry *123*, 117–133.

Liu, W., Cremer, J., Li, D., Hwa, T., and Liu, C. (2019). An evolutionarily stable strategy to colonize spatially extended habitats. Nature *575*, 664–668.

Lønborg, C., Middelboe, M., and Brussaard, C.P.D. (2013). Viral lysis of *Micromonas pusilla*: impacts on dissolved organic matter production and composition. Biogeochemistry *116*, 231–240.

Long, R.A., and Azam, F. (2001). Microscale patchiness of bacterioplankton assemblage richness in seawater. Aquat. Microb. Ecol. *26*, 103–113.

López-Pérez, M., Gonzaga, A., Martin-Cuadrado, A.-B., Onyshchenko, O., Ghavidel, A., Ghai, R., and Rodriguez-Valera, F. (2012). Genomes of surface isolates of *Alteromonas macleodii* : the life of a widespread marine opportunistic copiotroph. Sci. Rep. *2*, 696.

Luchsinger, R.H., Bergersen, B., and Mitchell, J.G. (1999). Bacterial swimming strategies and turbulence. Biophys. J. *77*, 2377–2386.

Lux, R., and Shi, W. (2004). Chemotaxis-guided movements in bacteria. Crit. Rev. Oral Biol. Med. Off. Publ. Am. Assoc. Oral Biol. *15*, 207–220.

Ma, X., Coleman, M.L., and Waldbauer, J.R. (2018). Distinct molecular signatures in dissolved organic matter produced by viral lysis of marine cyanobacteria. Environ. Microbiol. *20*, 3001–3011.

Macnab, R.M (1996). Flagella and motility. *Escherichia Coli* and *Salmonella*.

Macnab, R.M. (2003). How bacteria assemble flagella. Annu. Rev. Microbiol. *57*, 77–100.

Magariyama, Y., Sugiyama, S., Muramoto, K., Maekawa, Y., Kawagishi, I., Imae, Y., and Kudo, S. (1994). Very fast flagellar rotation. Nature *371*, 752–752.

Mandel, M.J., Schaefer, A.L., Brennan, C.A., Heath-Heckman, E.A.C., DeLoney-Marino, C.R., McFall-Ngai, M.J., and Ruby, E.G. (2012). Squid-derived chitin oligosaccharides are a chemotactic signal during colonization by *Vibrio fischeri*. Appl. Environ. Microbiol. *78*, 4620–4626.

Manson, M.D., Tedesco, P., Berg, H.C., Harold, F.M., and van der Drift, C. (1977). A protonmotive force drives bacterial flagella. Proc. Natl. Acad. Sci. *74*, 3060–3064.

Margulis, L. (1981). Symbiosis in cell evolution: Life and its environment on the early earth. San Francisco: Freeman.

Mari, X., Passow, U., Migon, C., Burd, A.B., and Legendre, L. (2017). Transparent exopolymer particles: effects on carbon cycling in the ocean. Prog. Oceanogr. *151*, 13–37.

Matanza, X.M., and Osorio, C.R. (2018). Transcriptome changes in response to temperature in the fish pathogen *Photobacterium damselae* subsp. *damselae*: Clues to understand the emergence of disease outbreaks at increased seawater temperatures. PLOS ONE *13*, e0210118.

Matz, C., and Jürgens, K. (2005). High motility reduces grazing mortality of planktonic bacteria. Appl. Environ. Microbiol. *71*, 921–929.

McCarren, J., and Brahamsha, B. (2007). SwmB, a 1.12-megadalton protein that is required for nonflagellar swimming motility in synechococcus. J. Bacteriol. *189*, 1158–1162.

McCarren, J., Heuser, J., Roth, R., Yamada, N., Martone, M., and Brahamsha, B. (2005). Inactivation of S*wmA* results in the loss of an outer cell layer in a swimming *Synechococcus* strain. J. Bacteriol. *187*, 224–230.

McCarren, J., Becker, J.W., Repeta, D.J., Shi, Y., Young, C.R., Malmstrom, R.R., Chisholm, S.W., and DeLong, E.F. (2010). Microbial community transcriptomes reveal microbes and metabolic pathways associated with dissolved organic matter turnover in the sea. Proc. Natl. Acad. Sci. U. S. A. *107*, 16420–16427.

McCarthy, J.J., and Goldman, J.C. (1979). Nitrogenous nutrition of marine phytoplankton in nutrient-depleted waters. Science *203*, 670–672.

McEvoy, M.M., Bren, A., Eisenbach, M., and Dahlquist, F.W. (1999). Identification of the binding interfaces on CheY for two of its targets the phosphatase *CheZ* and the flagellar switch protein FliM11Edited by P. E. Wright. J. Mol. Biol. *289*, 1423–1433.

Middelboe, M. (2000). Bacterial Growth Rate and Marine Virus-Host Dynamics. Microb. Ecol. *40*, 114–124.

Middelboe, M., and Jørgensen, N.O.G. (2006). Viral lysis of bacteria: an important source of dissolved amino acids and cell wall compounds. J. Mar. Biol. Assoc. U. K. *86*, 605–612.

Miller, T.R., and Belas, R. (2004). Dimethylsulfoniopropionate metabolism by *Pfiesteria*-associated *Roseobacter* spp. Appl. Environ. Microbiol. *70*, 3383–3391.

Miller, T.R., and Belas, R. (2006). Motility is involved in *Silicibacter* sp. TM1040 interaction with dinoflagellates. Environ. Microbiol. *8*, 1648–1659.

Miller, T.R., Hnilicka, K., Dziedzic, A., Desplats, P., and Belas, R. (2004). Chemotaxis of *Silicibacter* sp. strain TM1040 toward dinoflagellate products. Appl. Environ. Microbiol. *70*, 4692–4701.

Minniti, G., Hagen, L.H., Porcellato, D., Jørgensen, S.M., Pope, P.B., and Vaaje-Kolstad, G. (2017). The skin-mucus microbial community of farmed atlantic salmon (*Salmo salar*). Front. Microbiol. *8*, 2043.

Mitchell, J.G. (1991). The influence of cell size on marine bacterial motility and energetics. Microb. Ecol. *22*, 227–238.

Mitchell, J.G., and Kogure, K. (2006). Bacterial motility: links to the environment and a driving force for microbial physics. FEMS Microbiol. Ecol. *55*, 3–16.

Mitchell, J.G., Okubo, A., and Fuhrman, J.A. (1985). Microzones surrounding phytoplankton form the basis for a stratified marine microbial ecosystem. Nature *316*, 58–59.

Mitchell, J.G., Pearson, L., Bonazinga, A., Dillon, S., Khouri, H., and Paxinos, R. (1995a). Long lag times and high velocities in the motility of natural assemblages of marine bacteria. Appl. Environ. Microbiol. *61*, 877–882.

Mitchell, J.G., Pearson, L., Dillon, S., and Kantalis, K. (1995b). Natural assemblages of marine bacteria exhibiting high-speed motility and large accelerations. Appl. Env. Microbiol. *61*, 5.

Mitchell, J.G., Pearson, L., and Dillon, S. (1996). Clustering of marine bacteria in seawater enrichments. Appl. Environ. Microbiol. *62*, 3716–3721.

Mittelviefhaus, M., Müller, D.B., Zambelli, T., and Vorholt, J.A. (2019). A modular atomic force microscopy approach reveals a large range of hydrophobic adhesion forces among bacterial members of the leaf microbiota. ISME J. *13*, 1878–1882.

Møller, E.F. (2005). Sloppy feeding in marine copepods: prey-size-dependent production of dissolved organic carbon. J. Plankton Res. *27*, 27–35.

Möller, K.O., John, M.S., Temming, A., Floeter, J., Sell, A.F., Herrmann, J.-P., and Möllmann, C. (2012). Marine snow, zooplankton and thin layers: indications of a trophic link from small-scale sampling with the Video Plankton Recorder. Mar. Ecol. Prog. Ser. *468*, 57–69.

Moore, E.R., Davie-Martin, C.L., Giovannoni, S.J., and Halsey, K.H. (2020). *Pelagibacter* metabolism of diatom-derived volatile organic compounds imposes an energetic tax on photosynthetic carbon fixation. Environ. Microbiol. *22*, 1720–1733.

Moore, L.R., Rocap, G., and Chisholm, S.W. (1998). Physiology and molecular phylogeny of coexisting *Prochlorococcus* ecotypes. Nature *393*, 464–467.

Mopper, K., Schultz, C.A., Chevolot, L., Germain, C., Revuelta, R., and Dawson, R. (1992). Determination of sugars in unconcentrated seawater and other natural waters by liquid chromatography and pulsed amperometric detection. Environ. Sci. Technol. *26*, 133–138.

Moran, M.A., Buchan, A., González, J.M., Heidelberg, J.F., Whitman, W.B., Kiene, R.P., Henriksen, J.R., King, G.M., Belas, R., Fuqua, C., et al. (2004). Genome sequence of *Silicibacter pomeroyi* reveals adaptations to the marine environment. Nature *432*, 910–913.

Moran, M.A., Kujawinski, E.B., Stubbins, A., Fatland, R., Aluwihare, L.I., Buchan, A., Crump, B.C., Dorrestein, P.C., Dyhrman, S.T., Hess, N.J., et al. (2016). Deciphering ocean carbon in a changing world. Proc. Natl. Acad. Sci. *113*, 3143–3151.

Moriarty, D.J.W., Iverson, R.L., and Pollard, P.C. (1986). Exudation of organic carbon by the seagrass *Halodule wrightii* Aschers. And its effect on bacterial growth in the sediment. J. Exp. Mar. Biol. Ecol. *96*, 115–126.

Morris, R.M., Rappé, M.S., Connon, S.A., Vergin, K.L., Siebold, W.A., Carlson, C.A., and Giovannoni, S.J. (2002). SAR11 clade dominates ocean surface bacterioplankton communities. Nature *420*, 806–810.

Mühlenbruch, M., Grossart, H.-P., Eigemann, F., and Voss, M. (2018). Mini-review: phytoplankton-derived polysaccharides in the marine environment and their interactions with heterotrophic bacteria. Environ. Microbiol. *20*, 2671–2685.

Muramoto, K., Kawagishi, I., Kudo, S., Magariyama, Y., Imae, Y., and Homma, M. (1995). High-speed rotation and speed stability of the sodium-driven flagellar motor in *Vibrio alginolyticus*. J. Mol. Biol. *251*, 50–58.

Ni, B., Colin, R., Link, H., Endres, R.G., and Sourjik, V. (2020). Growth-rate dependent resource investment in bacterial motile behavior quantitatively follows potential benefit of chemotaxis. Proc. Natl. Acad. Sci. *117*, 595–601.

Nyholm, S.V., and McFall-Ngai, M. (2004). The winnowing: establishing the squid– *vibrio* symbiosis. Nat. Rev. Microbiol. *2*, 632–642.

Nyholm, S.V., Stabb, E.V., Ruby, E.G., and McFall-Ngai, M.J. (2000). Establishment of an animal–bacterial association: Recruiting symbiotic *vibrios* from the environment. Proc. Natl. Acad. Sci. *97*, 10231–10235.

Ochman, H., and Moran, N.A. (2001). Genes lost and genes found: evolution of bacterial pathogenesis and symbiosis. Science *292*, 1096–1099.

Ochsenkühn, M. A., Schmitt-Kopplin, P., Harir, M. and Amin, S.A., 2018. Coral metabolite gradients affect microbial community structures and act as a disease cue. Communications Biology, *1*, 1-10.

Ogawa, H., Amagai, Y., Koike, I., Kaiser, K., and Benner, R. (2001). Production of refractory dissolved organic matter by bacteria. Science *292*, 917–920.

Osterholz, H., Niggemann, J., Giebel, H.-A., Simon, M., and Dittmar, T. (2015). Inefficient microbial production of refractory dissolved organic matter in the ocean. Nat. Commun. *6*, 7422.

Overmann, J., and Lepleux, C. (2016). Marine bacteria and archaea: diversity, adaptations, and culturability. In the Marine Microbiome: An untapped source of biodiversity and biotechnological potential, L.J. Stal, and M.S. Cretoiu, eds. (Cham: Springer International Publishing), pp. 21–55.

Paerl, H.W., and Prufert, L.E. (1987). Oxygen-poor microzones as potential sites of microbial $N_2$ fixation in nitrogen-depleted aerobic marine waters. Appl. Environ. Microbiol. *53*, 1078–1087.

Panagiotopoulos, C., Pujo-Pay, M., Benavides, M., Van Wambeke, F., and Sempere, R. (2019). The composition and distribution of semi-labile dissolved organic matter across the southwest Pacific. Biogeosciences *16*, 105–116.

Passow, U. (2002). Production of transparent exopolymer particles (TEP) by phyto- and bacterioplankton. Mar. Ecol. Prog. Ser. *236*, 1–12.

Paul, J.H., DeFlaun, M.F., and Jeffrey, W.H. (1986). Elevated levels of microbial activity in the coral surface microlayer. Mar. Ecol. Prog. Ser. *33*, 29–40.

Pedersen, J.N., Bombar, D., Paerl, R.W., and Riemann, L. (2018). Diazotrophs and $N_2$-fixation associated with particles in coastal estuarine waters. Front. Microbiol. *9*, 2759.

Peduzzi, P., and Herndl, G.J. (1992). Zooplankton activity fueling the microbial loop: differential growth response of bacteria from oligotrophic and eutrophic waters. Limnol. Oceanogr. *37*, 1087–1092.

Petroff, A., and Libchaber, A. (2014). Hydrodynamics and collective behavior of the tethered bacterium *Thiovulum majus*. Proc. Natl. Acad. Sci. *111*, E537–E545.

Petroff, A.P., Wu, X.-L., and Libchaber, A. (2015). Fast-moving bacteria self-organize into active two-dimensional crystals of rotating cells. Phys. Rev. Lett. *114*, 158102.

Philippot, L., Raaijmakers, J.M., Lemanceau, P., and van der Putten, W.H. (2013). Going back to the roots: the microbial ecology of the rhizosphere. Nat. Rev. Microbiol. *11*, 789–799.

Ping, L., Birkenbeil, J., and Monajembashi, S. (2013). Swimming behavior of the monotrichous bacterium *Pseudomonas fluorescens* SBW25. FEMS Microbiol. Ecol. *86*, 36–44.

Ploug, H., and Grossart, H.-P. (2000). Bacterial growth and grazing on diatom aggregates: Respiratory carbon turnover as a function of aggregate size and sinking velocity. Limnol. Oceanogr. *45*, 1467–1475.

Pogoreutz, C., Voolstra, C.R., Rädecker, N., Weis, V., Cardenas, A., and Raina, J.-B. (2021). The coral holobiont highlights the dependence of cnidarian animal hosts on their associated microbes. Cellular Dialogues in the Holobiont, CRC Press. 91-118

Pollock, F.J., McMinds, R., Smith, S., Bourne, D.G., Willis, B.L., Medina, M., Thurber, R.V., and Zaneveld, J.R. (2018). Coral-associated bacteria demonstrate phylosymbiosis and cophylogeny. Nat. Commun. *9*, 4921.

Poretsky, R.S., Sun, S., Mou, X., and Moran, M.A. (2010). Transporter genes expressed by coastal bacterioplankton in response to dissolved organic carbon. Environ. Microbiol. *12*, 616–627.

Purcell, E.M. (1977). Life at low Reynolds number. Am. J. Phys. *45*, 3–11.

Purcell, E.M. (1997). The efficiency of propulsion by a rotating flagellum. Proc. Natl. Acad. Sci. *94*, 11307–11311.

Quax, T.E.F., Altegoer, F., Rossi, F., Li, Z., Rodriguez-Franco, M., Kraus, F., Bange, G., and Albers, S.-V. (2018). Structure and function of the archaeal response regulator CheY. Proc. Natl. Acad. Sci. *115*, E1259–E1268.

Quelas, J.I., Althabegoiti, M.J., Jimenez-Sanchez, C., Melgarejo, A.A., Marconi, V.I., Mongiardini, E.J., Trejo, S.A., Mengucci, F., Ortega-Calvo, J.-J., and Lodeiro, A.R. (2016). Swimming performance of *Bradyrhizobium diazoefficiens* is an emergent property of its two flagellar systems. Sci. Rep. *6*, 23841.

Rahav, E., Giannetto, M.J., and Bar-Zeev, E. (2016). Contribution of mono and polysaccharides to heterotrophic $N_2$ fixation at the eastern Mediterranean coastline. Sci. Rep. *6*, 27858.

Raina, J.-B., Fernandez, V., Lambert, B., Stocker, R., and Seymour, J.R. (2019). The role of microbial motility and chemotaxis in symbiosis. Nat. Rev. Microbiol. *17*, 284–294.

Ramsing, N.B., Kühl, M., and Jørgensen, B.B. (1993). Distribution of sulfate-reducing bacteria, $O_2$, and $H_2S$ in photosynthetic biofilms determined by oligonucleotide probes and microelectrodes. Appl. Environ. Microbiol. *59*, 3840–3849.

Riemann, L., and Middelboe, M. (2002). Viral lysis of marine bacterioplankton: implications for organic matter cycling and bacterial clonal composition. Ophelia *56*, 57–68.

Riemann, L., Steward, G.F., and Azam, F. (2000). Dynamics of bacterial community composition and activity during a mesocosm diatom bloom. Appl. Environ. Microbiol. *66*, 578–587.

Rinke, C., Rubino, F., Messer, L.F., Youssef, N., Parks, D.H., Chuvochina, M., Brown, M., Jeffries, T., Tyson, G.W., Seymour, J.R., et al. (2019). A phylogenomic and ecological analysis of the globally abundant Marine Group II archaea ( Ca . Poseidoniales ord. nov.). ISME J. *13*, 663–675.

Rohwer, F., Breitbart, M., Jara, J., Azam, F., and Knowlton, N. (2001). Diversity of bacteria associated with the Caribbean coral *Montastraea franksi*. Coral Reefs *20*, 85–91.

Rohwer, F., Seguritan, V., Azam, F., and Knowlton, N. (2002). Diversity and distribution of coral-associated bacteria. Mar. Ecol. Prog. Ser. *243*, 1–10.

Rossel, P.E., Bienhold, C., Boetius, A., and Dittmar, T. (2016). Dissolved organic matter in pore water of Arctic Ocean sediments: environmental influence on molecular composition. Org. Geochem. *97*, 41–52.

Ruby, E.G., Urbanowski, M., Campbell, J., Dunn, A., Faini, M., Gunsalus, R., Lostroh, P., Lupp, C., McCann, J., Millikan, D., et al. (2005). Complete genome sequence of *Vibrio fischeri*: A symbiotic bacterium with pathogenic congeners. Proc. Natl. Acad. Sci. U. S. A. *102*, 3004–3009.

Rusch, D.B., Halpern, A.L., Sutton, G., Heidelberg, K.B., Williamson, S., Yooseph, S., Wu, D., Eisen, J.A., Hoffman, J.M., Remington, K., et al. (2007). The Sorcerer II Global Ocean Sampling Expedition: Northwest Atlantic through Eastern Tropical Pacific. PLOS Biol. *5*, e77.

Saba, G.K., Steinberg, D.K., and Bronk, D.A. (2011). The relative importance of sloppy feeding, excretion, and fecal pellet leaching in the release of dissolved carbon and nitrogen by *Acartia tonsa* copepods. J. Exp. Mar. Biol. Ecol. *404*, 47–56.

Salah Ud-Din, A.I.M., and Roujeinikova, A. (2017). Methyl-accepting chemotaxis proteins: a core sensing element in prokaryotes and archaea. Cell. Mol. Life Sci. *74*, 3293–3303.

Salek, M.M., Carrara, F., Fernandez, V., Guasto, J.S., and Stocker, R. (2019). Bacterial chemotaxis in a microfluidic T-maze reveals strong phenotypic heterogeneity in chemotactic sensitivity. Nat. Commun. *10*, 1877.

Sar, N., and Rosenberg, E. (1987). Fish skin bacteria: colonial and cellular hydrophobicity. Microb. Ecol. *13*, 193–202.

Schlesner, M., Miller, A., Streif, S., Staudinger, W.F., Müller, J., Scheffer, B., Siedler, F., and Oesterhelt, D. (2009). Identification of archaea-specific chemotaxis proteins which interact with the flagellar apparatus. BMC Microbiol. *9*, 56.

Schuech, R., Hoehfurtner, T., Smith, D.J. and Humphries, S., 2019. Motile curved bacteria are Pareto-optimal. PNAS. *116*(29), 14440-14447.

Schulz, H.N., and Jørgensen, B.B. (2001). Big bacteria. Annu. Rev. Microbiol. *55*, 105–137.

Segall, J.E., Manson, M.D., and Berg, H.C. (1982). Signal processing times in bacterial chemotaxis. Nature *296*, 855–857.

Segall, J.E., Block, S.M., and Berg, H.C. (1986). Temporal comparisons in bacterial chemotaxis. Proc. Natl. Acad. Sci. *83*, 8987–8991.

Seyedsayamdost, M.R., Case, R.J., Kolter, R., and Clardy, J. (2011). The Jekyll-and-Hyde chemistry of *Phaeobacter gallaeciensis*. Nat. Chem. *3*, 331–335.

Seymour, J.R., Mitchell, J.G., Pearson, L., and Waters, R.L. (2000). Heterogeneity in bacterioplankton abundance from 4.5 millimetre resolution sampling. Aquat. Microb. Ecol. *22*, 143–153.

Seymour, J.R., Marcos, and Stocker, R. (2009a). Resource patch formation and exploitation throughout the marine microbial food web. Am. Nat. *173*, E15–E29.

Seymour, J.R., Ahmed, T., and Stocker, R. (2009b). Bacterial chemotaxis towards the extracellular products of the toxic phytoplankton *Heterosigma akashiwo*. J. Plankton Res. *31*, 1557–1561.

Seymour, J.R., Simó, R., Ahmed, T., and Stocker, R. (2010a). Chemoattraction to dimethylsulfoniopropionate throughout the marine microbial food web. Science *329*, 342–345.

Seymour, J.R., Ahmed, T., Durham, W.M., and Stocker, R. (2010b). Chemotactic response of marine bacteria to the extracellular products of *Synechococcus* and *Prochlorococcus*. Aquat. Microb. Ecol. *59*, 161–168.

Seymour, J.R., Amin, S.A., Raina, J.-B., and Stocker, R. (2017). Zooming in on the phycosphere: the ecological interface for phytoplankton–bacteria relationships. Nat. Microbiol. *2*, 1–12.

Shahapure, R., Driessen, R.P.C., Haurat, M.F., Albers, S.-V., and Dame, R.T. (2014). The archaellum: a rotating type IV pilus. Mol. Microbiol. *91*, 716–723.

Shi, Y., McCarren, J., and DeLong, E.F. (2012). Transcriptional responses of surface water marine microbial assemblages to deep-sea water amendment. Environ. Microbiol. *14*, 191–206.

Shigematsu, M., Meno, Y., Misumi, H., and Amako, K. (1995). The measurement of swimming velocity of *Vibrio cholerae* and *Pseudomonas aeruginosa* using the video tracking method. Microbiol. Immunol. *39*, 741–744.

Shoemaker, K.M., Duhamel, S., and Moisander, P.H. (2019). Copepods promote bacterial community changes in surrounding seawater through farming and nutrient enrichment. Environ. Microbiol. *21*, 3737–3750.

Shotts, E.B., Albert, T.F., Wooley, R.E., and Brown, J. (1990). Microflora associated with the skin of the bowhead whale (*balaena mysticetus*). J. Wildl. Dis. *26*, 351–359.

Sievert, S.M., Kiene, R.P., and Schulz-Vogt, H.N. (2007). The sulfur cycle. Oceanography *20*, 117–123.

Silverman, M., and Simon, M. (1974). Flagellar rotation and the mechanism of bacterial motility. Nature *249*, 73–74.

Simó, R. (2001). Production of atmospheric sulfur by oceanic plankton: biogeochemical, ecological and evolutionary links. Trends Ecol. Evol. *16*, 287–294.

Simon, M., Grossart, H.-P., Schweitzer, B., and Ploug, H. (2002). Microbial ecology of organic aggregates in aquatic ecosystems. Aquat. Microb. Ecol. *28*, 175–211.

Słomka, J., and Stocker, R. (2020). Bursts characterize coagulation of rods in a quiescent fluid. Phys. Rev. Lett. *124*, 258001.

Słomka, J., Alcolombri, U., Secchi, E., Stocker, R., and Fernandez, V.I. (2020). Encounter rates between bacteria and small sinking particles. New J. Phys. *22*, 043016.

Smith, D.C., Simon, M., Alldredge, A.L., and Azam, F. (1992). Intense hydrolytic enzyme activity on marine aggregates and implications for rapid particle dissolution. Nature *359*, 139–142.

Smriga, S., Fernandez, V.I., Mitchell, J.G., and Stocker, R. (2016). Chemotaxis toward phytoplankton drives organic matter partitioning among marine bacteria. Proc. Natl. Acad. Sci. *113*, 1576–1581.

Son, K., Guasto, J.S., and Stocker, R. (2013). Bacteria can exploit a flagellar buckling instability to change direction. Nat. Phys. *9*, 494–498.

Son, K., Menolascina, F., and Stocker, R. (2016). Speed-dependent chemotactic precision in marine bacteria. Proc. Natl. Acad. Sci. *113*, 8624–8629.

Sonnenschein, E.C., Syit, D.A., Grossart, H.-P., and Ullrich, M.S. (2012). Chemotaxis of *Marinobacter adhaerens* and its impact on attachment to the diatom *Thalassiosira weissflogii*. Appl. Environ. Microbiol. *78*, 6900–6907.

Sourjik, V., and Berg, H.C. (2002a). Receptor sensitivity in bacterial chemotaxis. Proc. Natl. Acad. Sci. *99*, 123-127.

Sourjik, V., and Berg, H.C. (2002b). Binding of the *Escherichia coli* response regulator CheY to its target measured in vivo by fluorescence resonance energy transfer. Proc. Natl. Acad. Sci. *99*, 12669–12674.

Stocker, R. (2011). Reverse and flick: Hybrid locomotion in bacteria. Proc. Natl. Acad. Sci. *108*, 2635-2636.

Stocker, R. (2012). Marine microbes see a sea of gradients. Science *338*, 628–633.

Stocker, R. (2015). The 100 µm length scale in the microbial ocean. Aquat. Microb. Ecol. *76*, 189–194.

Stocker, R., and Seymour, J.R. (2012). Ecology and physics of bacterial chemotaxis in the ocean. Microbiol. Mol. Biol. Rev. MMBR *76*, 792–812.

Stocker, R., Seymour, J.R., Samadani, A., Hunt, D.E., and Polz, M.F. (2008). Rapid chemotactic response enables marine bacteria to exploit ephemeral microscale nutrient patches. Proc. Natl. Acad. Sci. U. S. A. *105*, 4209–4214.

Streif, S., Staudinger, W.F., Marwan, W., and Oesterhelt, D. (2008). Flagellar rotation in the archaeon *Halobacterium salinarum* depends on ATP. J. Mol. Biol. *384*, 1–8.

Sunagawa, S., Coelho, L.P., Chaffron, S., Kultima, J.R., Labadie, K., Salazar, G., Djahanschiri, B., Zeller, G., Mende, D.R., Alberti, A., et al. (2015). Structure and function of the global ocean microbiome. Science *348*, 1261359.

Suttle, C.A. (1994). The significance of viruses to mortality in aquatic microbial communities. Microb. Ecol. *28*, 237–243.

Suttle, C.A. (2007). Marine viruses — major players in the global ecosystem. Nat. Rev. Microbiol. *5*, 801–812.

Suttle, C.A., and Chan, A.M. (1994). Dynamics and distribution of cyanophages and their effect on marine *Synechococcus* spp. Appl. Environ. Microbiol. *60*, 3167–3174.

Tang, K.W. (2005). Copepods as microbial hotspots in the ocean: effects of host feeding activities on attached bacteria. Aquat. Microb. Ecol. *38*, 31–40.

Taylor, J.D., and Cunliffe, M. (2017). Coastal bacterioplankton community response to diatom-derived polysaccharide microgels. Environ. Microbiol. Rep. *9*, 151–157.

Taylor, J.R., and Stocker, R. (2012). Trade-offs of chemotactic foraging in turbulent water. Science *338*, 675–679.

Taylor, M.W., Radax, R., Steger, D., and Wagner, M. (2007). Sponge-associated microorganisms: evolution, ecology, and biotechnological Potential. Microbiol. Mol. Biol. Rev. *71*, 295–347.

Teeling, H., Fuchs, B.M., Bennke, C.M., Krüger, K., Chafee, M., Kappelmann, L., Reintjes, G., Waldmann, J., Quast, C., Glöckner, F.O., et al. (2016). Recurring patterns in bacterioplankton dynamics during coastal spring algae blooms. ELife *5*, e11888.

Thar, R., and Kühl, M. (2002). Conspicuous veils formed by vibrioid bacteria on sulfidic marine sediment. Appl. Environ. Microbiol. *68*, 6310–6320.

Thar, R., and Kühl, M. (2003). Bacteria are not too small for spatial sensing of chemical gradients: an experimental evidence. Proc. Natl. Acad. Sci. *100*, 5748–5753.

Thomas, N.A., Bardy, S.L., and Jarrell, K.F. (2001). The archaeal flagellum: a different kind of prokaryotic motility structure. FEMS Microbiol. Rev. *25*, 147–174.

Thomas, T., Evans, F.F., Schleheck, D., Mai-Prochnow, A., Burke, C., Penesyan, A., Dalisay, D.S., Stelzer-Braid, S., Saunders, N., Johnson, J., et al. (2008). Analysis of the *Pseudoalteromonas tunicata* genome reveals properties of a surface-associated life style in the marine environment. PLOS ONE *3*, e3252.

Thornton, D.C.O. (2014). Dissolved organic matter (DOM) release by phytoplankton in the contemporary and future ocean. Eur. J. Phycol. *49*, 20–46.

Thornton, K.L., Butler, J.K., Davis, S.J., Baxter, B.K., and Wilson, L.G. (2020). Haloarchaea swim slowly for optimal chemotactic efficiency in low nutrient environments. Nat. Commun. *11*, 4453.

Tout, J., Jeffries, T.C., Webster, N.S., Stocker, R., Ralph, P.J., and Seymour, J.R. (2014). Variability in microbial community composition and function between different niches within a coral reef. Microb. Ecol. *67*, 540–552.

Tout, J., Jeffries, T.C., Petrou, K., Tyson, G.W., Webster, N.S., Garren, M., Stocker, R., Ralph, P.J., and Seymour, J.R. (2015). Chemotaxis by natural populations of coral reef bacteria. ISME J. *9*, 1764–1777.

Tripp, H.J., Kitner, J.B., Schwalbach, M.S., Dacey, J.W.H., Wilhelm, L.J., and Giovannoni, S.J. (2008). SAR11 marine bacteria require exogenous reduced sulphur for growth. Nature *452*, 741–744.

Trolldenier, G. (1987). Curl, E.A. and B. Truelove: The Rhizosphere. (Advanced Series in Agricultural Sciences, Vol. 15) Springer-Verlag, Berlin-Heidelberg-New York-Tokyo, 1986. 288 p, 57 figs., Hardcover DM 228.00, ISBN 3–540–15803–0. Z. Für Pflanzenernähr. Bodenkd. *150*, 124–125.

Tsai, C.-L., Tripp, P., Sivabalasarma, S., Zhang, C., Rodriguez-Franco, M., Wipfler, R.L., Chaudhury, P., Banerjee, A., Beeby, M., Whitaker, R.J., et al. (2020). The structure of the periplasmic FlaG–FlaF complex and its essential role for archaellar swimming motility. Nat. Microbiol. *5*, 216–225.

Tully, B.J. (2019). Metabolic diversity within the globally abundant Marine Group II Euryarchaea offers insight into ecological patterns. Nat. Commun. *10*, 271.

Turner, R.D., Hobbs, J.K., and Foster, S.J. (2016). Atomic force microscopy analysis of bacterial cell wall peptidoglycan architecture. In Bacterial Cell Wall Homeostasis: Methods and Protocols, H.-J. Hong, ed. (New York, NY: Springer), pp. 3–9.

van Tol, H.M., Amin, S.A., and Armbrust, E.V. (2017). Ubiquitous marine bacterium inhibits diatom cell division. ISME J. *11*, 31–42.

Vega Thurber, R., Willner-Hall, D., Rodriguez-Mueller, B., Desnues, C., Edwards, R.A., Angly, F., Dinsdale, E., Kelly, L., and Rohwer, F. (2009). Metagenomic analysis of stressed coral holobionts. Environ. Microbiol. *11*, 2148–2163.

Venter, J.C., Remington, K., Heidelberg, J.F., Halpern, A.L., Rusch, D., Eisen, J.A., Wu, D., Paulsen, I., Nealson, K.E., Nelson, W., et al. (2004). Environmental genome shotgun sequencing of the Sargasso Sea. Science *304*, 66–74.

Vila-Costa, M., Rinta-Kanto, J.M., Sun, S., Sharma, S., Poretsky, R., and Moran, M.A. (2010). Transcriptomic analysis of a marine bacterial community enriched with dimethylsulfoniopropionate. ISME J. *4*, 1410–1420.

Visser, A.W., and Jackson, G.A. (2004). Characteristics of the chemical plume behind a sinking particle in a turbulent water column. Mar. Ecol. Prog. Ser. *283*, 55–71.

Vorobev, A., Sharma, S., Yu, M., Lee, J., Washington, B.J., Whitman, W.B., Ballantyne, F., Medeiros, P.M., and Moran, M.A. (2018). Identifying labile DOM components in a coastal ocean through depleted bacterial transcripts and chemical signals. Environ. Microbiol. *20*, 3012–3030.

Wadhams, G.H., and Armitage, J.P. (2004). Making sense of it all: bacterial chemotaxis. Nat. Rev. Mol. Cell Biol. *5*, 1024–1037.

Watrous, J., Roach, P., Alexandrov, T., Heath, B.S., Yang, J.Y., Kersten, R.D., van der Voort, M., Pogliano, K., Gross, H., Raaijmakers, J.M., et al. (2012). Mass spectral molecular networking of living microbial colonies. Proc. Natl. Acad. Sci. *109*, E1743–E1752.

Watteaux, R., Stocker, R., and Taylor, J.R. (2015). Sensitivity of the rate of nutrient uptake by chemotactic bacteria to physical and biological parameters in a turbulent environment. J. Theor. Biol. *387*, 120–135.

Webster, N.S., and Taylor, M.W. (2012). Marine sponges and their microbial symbionts: love and other relationships. Environ. Microbiol. *14*, 335–346.

Webster, N.S., and Thomas, T. (2016). The sponge hologenome. MBio *7* (2).

Weinbauer, M., and Peduzzi, P. (1995). Effect of virus-rich high molecular weight concentrates of seawater on the dynamics of dissolved amino acids and carbohydrates. Mar. Ecol. Prog. Ser. *127*, 245–253.

Weiner, R.M., Ii, L.E.T., Henrissat, B., Hauser, L., Land, M., Coutinho, P.M., Rancurel, C., Saunders, E.H., Longmire, A.G., Zhang, H., et al. (2008). Complete genome sequence of the complex carbohydrate-degrading marine bacterium, *Saccharophagus degradans* Strain 2-40T. PLOS Genet. *4*, e1000087.

Wild, C., Huettel, M., Klueter, A., Kremb, S.G., Rasheed, M.Y.M., and Jørgensen, B.B. (2004). Coral mucus functions as an energy carrier and particle trap in the reef ecosystem. Nature *428*, 66–70.

Willey, J.M., and Waterbury, J.B. (1989). Chemotaxis toward nitrogenous compounds by swimming strains of marine *Synechococcus* spp. Appl. Environ. Microbiol. *55*, 1888–1894.

Williams, P.M., and Druffel, E.R.M. (1987). Radiocarbon in dissolved organic matter in the central North Pacific Ocean. Nature *330*, 246–248.

2175 Xie, L., Altindal, T., Chattopadhyay, S., and Wu, X.-L. (2011). Bacterial flagellum as a propeller and as a
2176 rudder for efficient chemotaxis. Proc. Natl. Acad. Sci. U. S. A. *108*, 2246–2251.

2177 Xu, T., Su, Y., Xu, Y., He, Y., Wang, B., Dong, X., Li, Y., and Zhang, X.-H. (2014). Mutations of
2178 flagellar genes *fliC12*, *fliA* and *flhDC* of *Edwardsiella tarda* attenuated bacterial motility, biofilm
2179 formation and virulence to fish. J. Appl. Microbiol. *116*, 236–244.

2180 Ya, V., Jw, D., Pa, J., and Bb, K.-B. (1998). A predictive model of bacterial foraging by means of freely
2181 released extracellular enzymes. Microb. Ecol. *36*, 75–92.

2182 Yang, Y., M. Pollard, A., Höfler, C., Poschet, G., Wirtz, M., Hell, R., and Sourjik, V. (2015). Relation
2183 between chemotaxis and consumption of amino acids in bacteria. Mol. Microbiol. *96*, 1272–1282.

2184 Yorimitsu, T., and Homma, M. (2001). Na+-driven flagellar motor of Vibrio. Biochim. Biophys. Acta
2185 BBA - Bioenerg. *1505*, 82–93.

2186 Zehr, J.P., Weitz, J.S., and Joint, I. (2017). How microbes survive in the open ocean. Science *357*, 646–
2187 647.

2188 Zhang, C., Dang, H., Azam, F., Benner, R., Legendre, L., Passow, U., Polimene, L., Robinson, C., Suttle,
2189 C.A., and Jiao, N. (2018). Evolving paradigms in biological carbon cycling in the ocean. Natl. Sci. Rev.
2190 *5*, 481–499.

2191 Ziegler, G.R., Benado, A.L., and Rizvi, S.S.H. (1987). Determination of mass diffusivity of simple sugars
2192 in water by the rotating disk method. J. Food Sci. *52*, 501–502.

2193 Zimmer-Faust, R.K., Souza, M.P. de, and Yoch, D.C. (1996). Bacterial chemotaxis and its potential role
2194 in marine dimethylsulfide production and biogeochemical sulfur cycling. Limnol. Oceanogr. *41*, 1330–
2195 1334.

2196